Nonlinear fuzzy observer for payload estimation in physical human-robot interaction

D. van Dieten
4028104

Master of Science Thesis

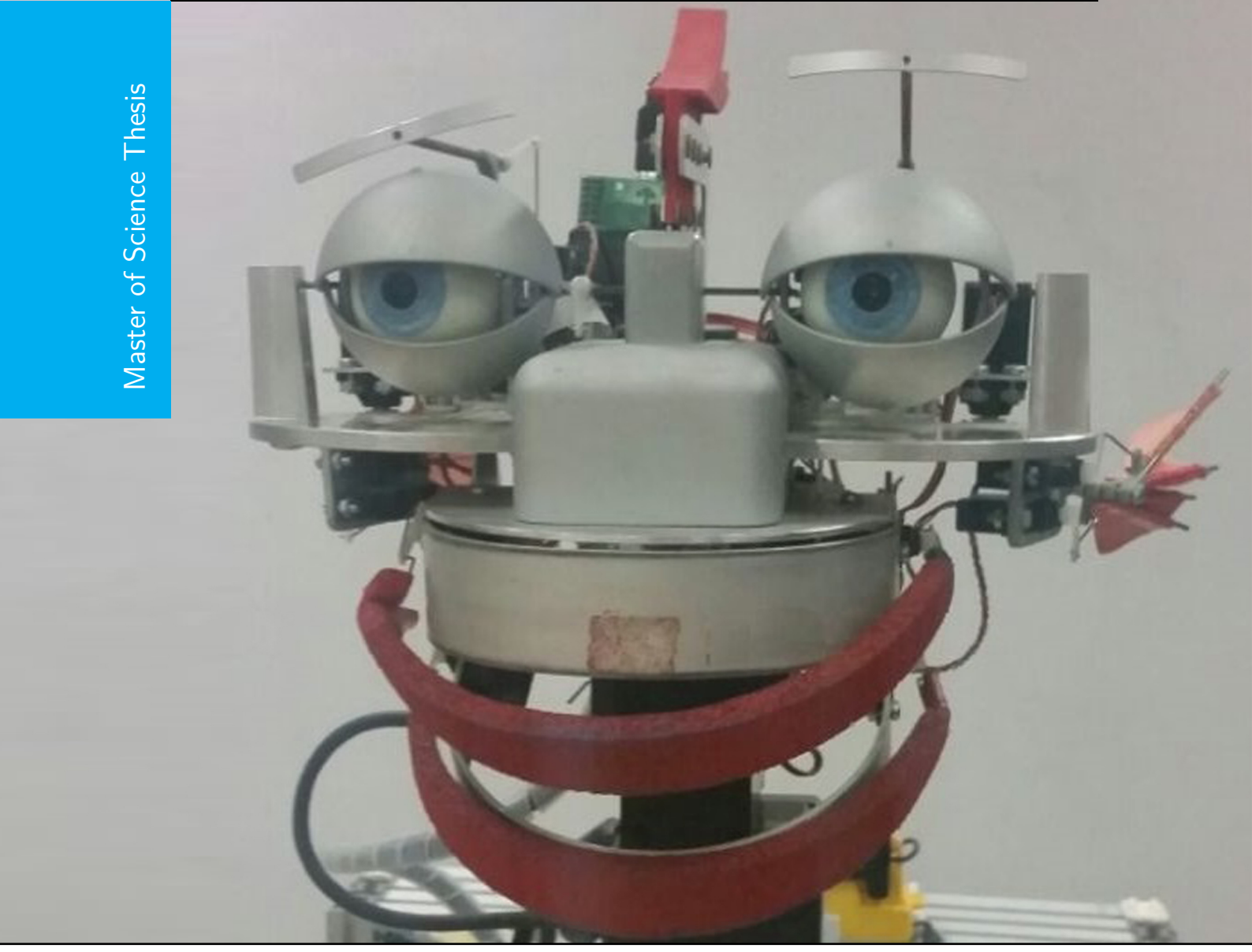

TU Delft Delft University of Technology

Delft Center for Systems and Control

Nonlinear fuzzy observer for payload estimation in physical human-robot interaction

Master of Science Thesis

For the degree of Master of Science in Mechanical Engineering - Control Engineering at Delft University of Technology

D. van Dieten
4028104

June 11, 2015

Faculty of Mechanical, Maritime and Materials Engineering (3ME) · Delft University of Technology

The information in this Literature Review is supported by KLM Cargo

Delft University of Technology
Department of
Delft Center for Systems and Control (dcsc)

The undersigned hereby certify that they have read and recommend to the Faculty of Mechanical, Maritime and Materials Engineering (3ME) for acceptance a thesis entitled

Nonlinear fuzzy observer for payload estimation in physical human-robot interaction

by

D. van Dieten
4028104

in partial fulfillment of the requirements for the degree of

Master of Science Mechanical Engineering - Control Engineering

Dated: June 11, 2015

Supervisor(s):

Prof.dr. R. Babuska

Reader(s):

Prof.dr.ir. Bart de Schutter

Ir. Wouter Wolfslag

Summary

Robotics have developed at a very high rate in the last few years. Industries are becoming capable of automating repetitive procedures without pause, and the production speed and quality are improving everyday. The main drawback of robotics in industry is the inability to deal with slight changes in an environment or in certain object parameters. This problem is very much present at Koninklijke Luchtvaart Maatschappij (KLM) Cargo, therefore they want to automate parts of their product handling cycle. KLM Cargo handles 540 000 tons of cargo every year and their processing hub is located at Schiphol airport. A number of automation opportunities exist at this location, such as the use of Automatic Guided Vehicle (AGV), smart planning algorithms and palletising/depalletising robots. This last point is addressed in this thesis.

The automation of the palletising/depalletising procedure is highly complex for a number of reasons: large variety of packages to be handled, restrictions for orientation of packages, hazardous materials, and more. The planning of a palletising order can handle the orientation problem and the placement of hazardous cargo, but the variety in size, weight and shape of packages makes fully automated palletising/depalletising difficult. The process of handling the packages is performed by manual labour and with the help of forklift trucks. An ideal solution to compensate the arduous labour is to use physical Human-Robot Interaction (pHRI). This concept allows a robot and human to handle cargo together to place it at a location. The current academic developments in human-robot collaborative object manipulation require known object dynamics and dimensions. This information is not known at KLM cargo, and therefore, the framework of human-robot collaborative object manipulation must be extended to allow for unknown object dynamics. One approach is currently being developed by using the Slotine and Li method of adaptive control. Unfortunately, this approach has a big drawback with regards to persistence of excitation. A new method utilizes fuzzy Takagi-Sugeno (TS) system with the sector nonlinearity approach where payload information is included in the systems state vector. This approach allows an observer to estimate the payload parameters without the persistence of excitation limitation. This thesis shows the motivation for using the fuzzy approach and develop it for a two-link manipulator and compare its performance to the classical approach.

While the classical approach works under persistence of excitation, a one link manipulator is

shown to work without this condition. Two fuzzy observers were tested, the fuzzy Luenberger observer and a sliding mode observer. Unfortunately, for the two link manipulator a feasible observer gain is not found. The approach was tested again, but this time only to estimate the mass of the payload. Unfortunately, this did not yield a feasible observer either. In order to find out the reason for this infeasibility and create an approach that will obtain a feasible solution requires more analysis of the observability of the fuzzy system.

Contents

Acknowledgements

I would like to thank my supervisor Prof.dr. R. Babuska for his assistance during the writing of this thesis. I would also like to thank the TUM, especially Sebastian Erhart and Prof. Dr.-Ing. Sandra Hirche for hosting me and helping me learn about pHRI. I want to thank Bart Krol and KLM CARGO for their support in developing this project.

Special thanks go out to Jessica for her support and for always believing in me. Also Sjak, Doret, Vivienne, Job for their never ending support and Andrea, Luca, and Joaquin for helping me during my period at Technische Universität München (TUM).

Chapter 1

Introduction

1-1 KLM cargo

Koninklijke Luchtvaart Maatschappij (KLM) is a Dutch airline business founded in 1919 whose first flight was from Amsterdam to London in 1920 carrying 345 passengers and 25 000 kilos of cargo in their first year. Much has changed since that period and as the oldest airline to have kept its original name, KLM fused with Air France in 2004, making the Air France - KLM group. Now KLM deals with 540 000 tons of cargo annually to 350 destinations. The KLM cargo department collaborates with the Air France cargo department to transport a whole range of goods separated into four services,

- General cargo
- Equation (Express cargo)
- VMA (Variation, Mail, Aerospace)
- Cohesion & Industries

The cargo bay of KLM, where the cargo is handled, is located at Amsterdam Airport Schiphol (SPL) beside the runway. Here the cargo bay has direct entry onto the runway to deliver the cargo directly to the plane. In Figure 1-1 the overview of the cargo bay on April 2014 is shown including the main areas within the departments. Shown are a number of special handling units such as the Safe, Animal Hotel and Aerospace, and the global sections Worldport 1 (WP1) & Worldport 2 (WP2), Europort and many more. The cargo bay is separated into three main buildings, Vrachtgebouw/Freightbuilding 1 (VG1/FB1), Vrachtgebouw/Freightbuilding 2 (VG2/FB2), and Vrachtgebouw/Freightbuilding 3 (VG3/FB3).

1-1-1 Vrachtgebouw/Freightbuilding 1 (VG1/FB1)

VG1/FB1 deals specifically with Variation and Equation. Airmail will come through this section to be sorted into destinations. All products in Equation are express cargo and require

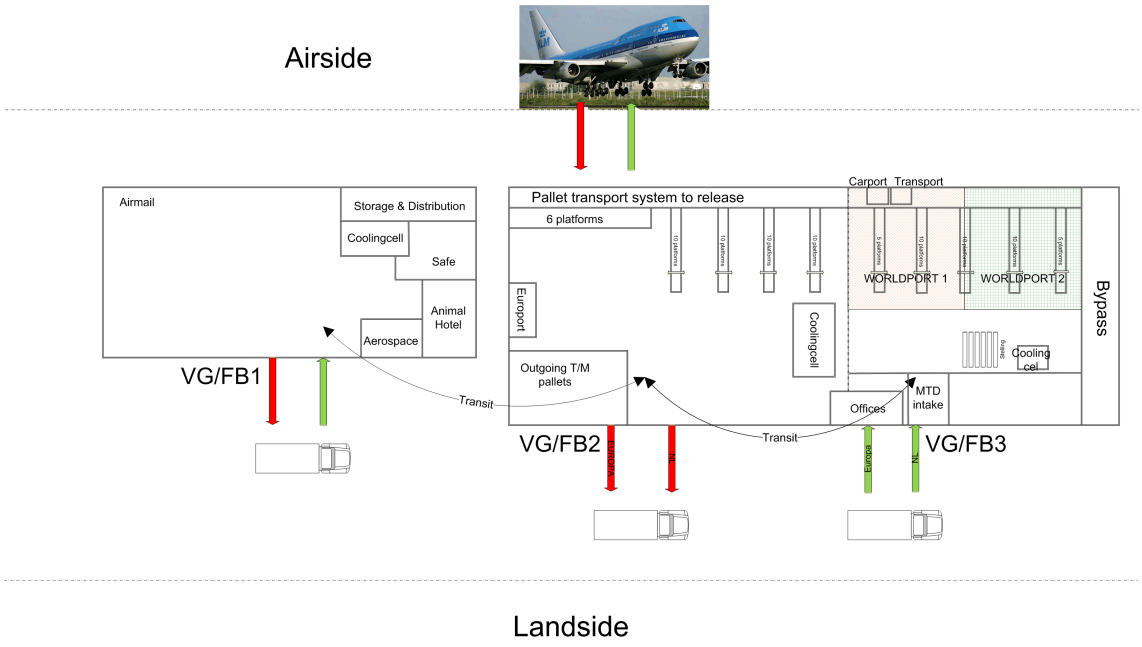

Figure 1-1: Cargo bay Layout

fast handling. There is a dedicated area in VG1/FB1 to handle this. Finally, VG1/FB1 has dedicated areas for animal transport, high valued goods and the aerospace sector. These last points will sometimes flow over into the other buildings to be grouped by destination if possible.

1-1-2 Vrachtgebouw/Freightbuilding 2 (VG2/FB2)

VG2/FB2 deals with incoming cargo. Cargo, loaded in aircraft pallets and/or containers (referred to as Unit Load Device (ULD)) from incoming flights is disassembled here and will be loaded onto trucks to be transported to the European destinations. The trucking destinations are separated into Europe (EUR) and Amsterdam (AMS) destinations. Figure 1-2 shows the cargo handling process [1]. In this flowchart two types of ULDs are handled, Mixed Unit Load Device (M-ULD) and True Unit Load Device (T-ULD). A T-ULD is a ULD which does not require any more loading or unloading and can simply be passed straight through to the truck or to VG3/FB3. Any freight which needs to be flown will be passed onto VG3. A M-ULD can be broken down at VG2/FB2 and the individual product will be either released to the trucking for local and European destinations, or sent to VG3/FB3 for rebuilding onto another ULD.

1-1-3 Vrachtgebouw/Freightbuilding 3 (VG3/FB3)

VG3/FB3 is the building with the most activity and work floor staff. Here the ULDs are built and broken down (same as VG2/FB2) for flights. This building has an intake section on the land side where trucks are unloaded and the cargo is moved to a Work Station (WS) to be built up for the flight. When the ULD is completed, it is released into the Pallet/Container

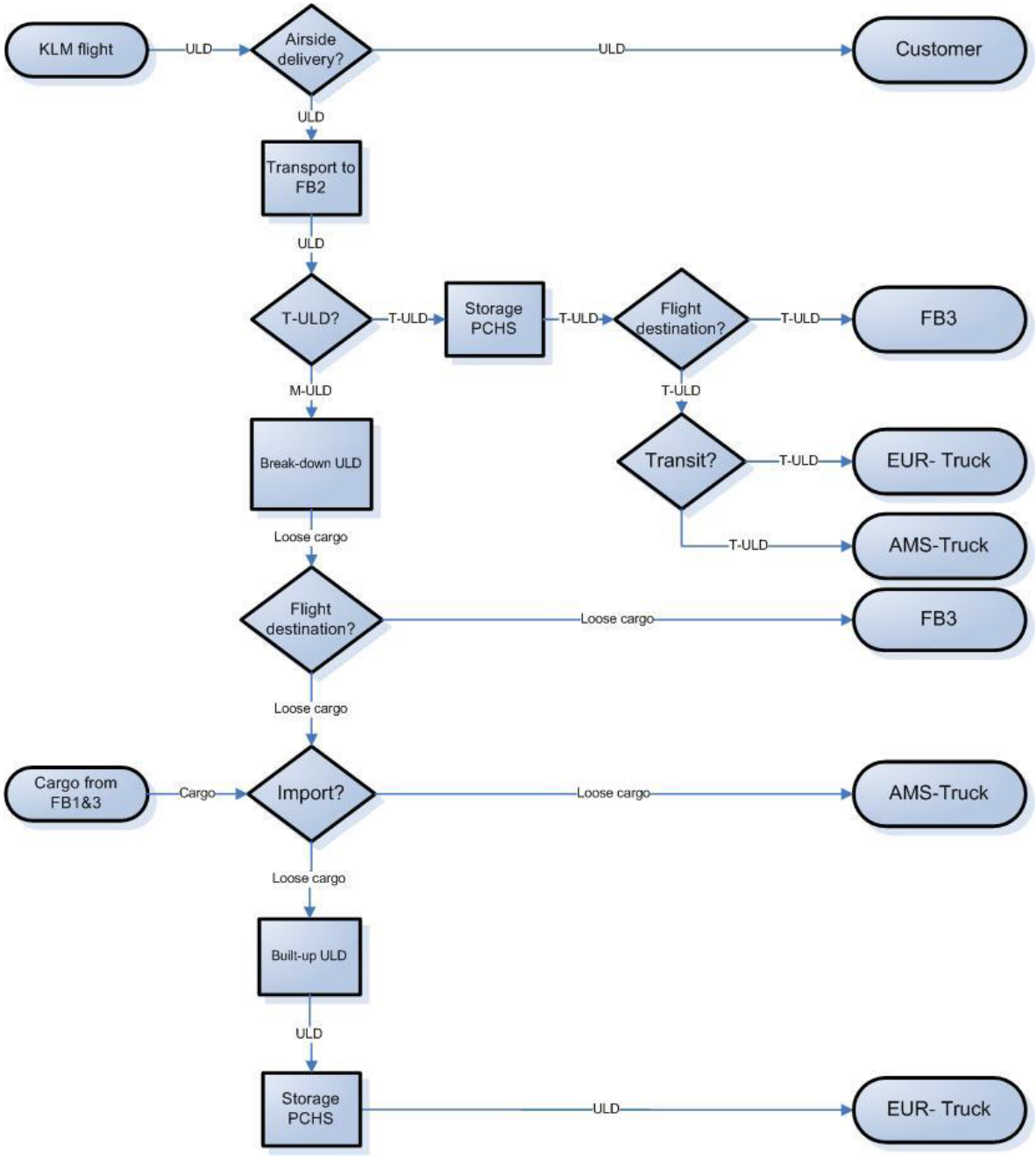

Figure 1-2: VG2/FB2 cargo handling process

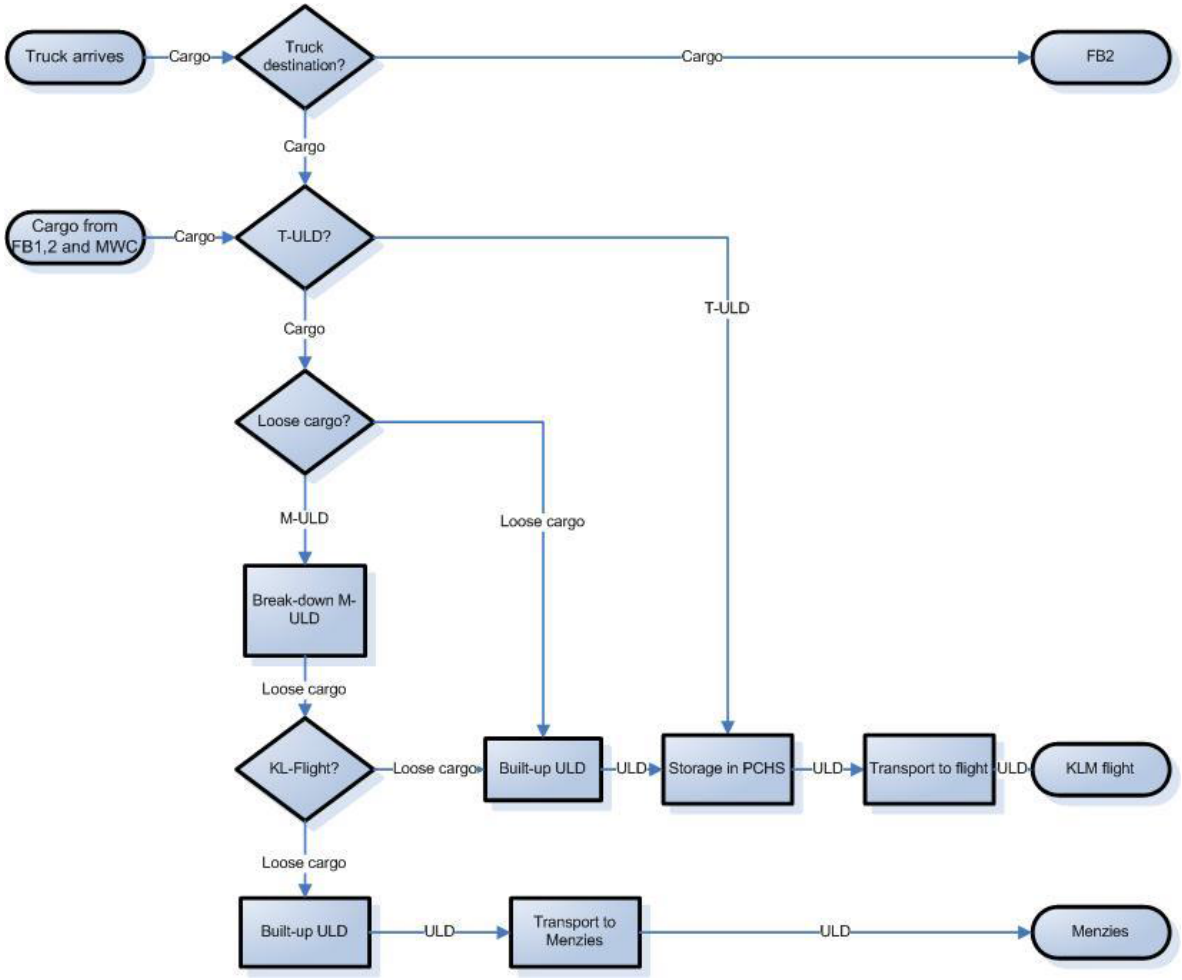

Figure 1-3: VG3/FB3 cargo handling process

Handling System (PCHS) and can be taken to the plane when necessary. Truck driven cargo is due to arrive between 2 and 5 hours before the flight is scheduled to depart (this time frame is not always achieved but is handled specially, or moved onto a different flight). Some ULDs are M-ULDs and are broken down and rebuilt by their new destination. This process happens in VG3/FB3. Between the different buildings there is some cross traffic. Some of the broken down products at VG2/FB2 are assigned to outgoing flights and are built up again at VG3/FB3. Some packages from VG1/FB1 are also included in the ULDs built in VG3/FB3. Transport between these facilities is often carried out by forklift trucks and sometimes small carriages with trailers.

1-1-4 ULD

A Unit Load Device (ULD) is an aircraft pallet/container standardised for all planes. Aircraft's are divided by their different types of cargo holds as shown in Figure 1-4.

Figure 1-4: Types of cargo holds on planes

- Cargo only
  - Main deck
  - Lower deck
  - Bulk
- PAX
  - Lower deck
  - Bulk
- Combi
  - Main deck (shared with passengers)
  - Lower deck
  - Bulk

The Bulk hold cannot take any ULDs, while the Main and Lower deck holds have different height restrictions for their ULD. Each aircraft has its own specifications as the Main and Lower deck ULDs can be built in such a way to follow the contours of the hold. KLM uses a number of different types of ULD as shown in Table 1-1 and Table 1-2 [2]. Each constructed ULD has its own specific usable volume and planned load. The amount of products placed on a pallet is a task shared between planners and the work floor staff. Each flight receives a number of allocated spots for ULDs and the received packages are planned per flight with a

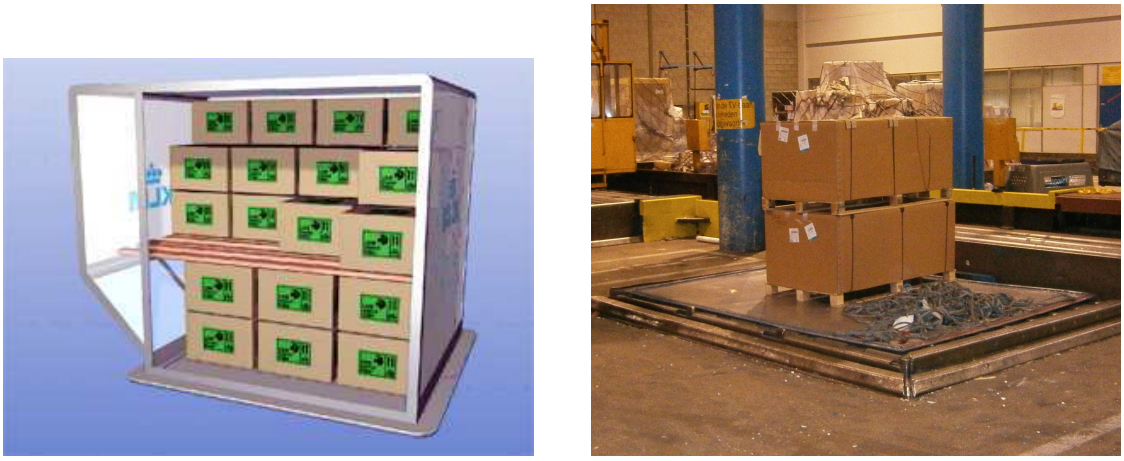

(a) Container **(b)** Pallet

Figure 1-5: ULD types

Table 1-1: Pallet ULD types

IATA code	Dimensions (L×W) (cm)	Tare weight (empty inc. net) (kg)
P1P/PAP/PAG	318 × 224	120
P6P/PQP/PMC	318 × 244	125
P4M/PZA/PRA	498 × 156	365
P7E/PSE/PGA	606 × 244	430
P9A/PLA/PLB	318 × 153	94

restricted number of ULDs. The types of ULD that may be used can be summed up into two groups, containers (Figure 1-5a) and pallets (Figure 1-5b). The main restriction of a container is the access possibilities. Most containers can only be accessed from one of the sides which is covered with a flexible plastic cover. Sometimes the overhang as shown in Figure 1-5a of the container is not directly accessible from the outside. The ULDs are limited not only by its length and width but also by its allowed weight. This limitation is defined by which position the ULD will take in the aicraft's cargo hold. Each plane is split into a number of subsections where cargo may be stored. These details are specified for specific positions within a specific type in the Aircraft Handling Manual (AHM)[2] and for each individual aircraft type within the Air France - KLM fleet ([3–12]). When planning the cargo which is to be built up onto a ULD, a planner will notify the workshop of which products will be loaded onto which ULD. The loading process of the ULDs is a palletising problem referred to as the Distributors Package Packing Problem (DPPP). This process at KLM can be further analysed.

1-1-5 Development options

The process as explained above does not make use of many automatic aids. The planning is completed using a number of different computer programs, but the movement of products

Table 1-2: Container ULD types

IATA code	Base Dimensions (L×W)(cm)	Body Dimensions (L×W×H)(cm)	Tare weight (kg)
AKE	156 × 153	200 × 151 × 162	65
RKN	156 × 153	200 × 151 × 162	267/635
AAF	318 × 224	404 × 224 × 161	270
AAK	318 × 224	317 × 223 × 161	250
AMF	318 × 244	404 × 244 × 161	305
AAP	318 × 224	318 × 224 × 162	219/286/240
RAP	318 × 224	318 × 224 × 162	438/1100

over the work floor is mainly performed by use of manual labour and fork lift trucks. A T-ULD is handled by a PCHS where a fully constructed ULD may be temporarily stored. This system ensures that ULDs arrive at the correct times to the correct outlet ports. After a careful mapping of the process, five improvement opportunities were identified:

- Automatic sorter for letters and small packages
- Weight, volume and dimension analysis before handling
- Smart tagging
- Automated product movement over work floor
- Automated palletising/depalletising
- Planning of ULD construction through algorithm (DPPP)

For the first four points, solutions exist in industry and can be implemented. Smart tagging may be achieved through the used of Radio Frequency Identification (RFID) scanning and the product movement may be achieved through the use of Automatic Guided Vehicle (AGV)s or conveyor systems. For the automated palletising/depalletising there are limited possibilities. To analyse the opportunities in this option, the current process must be analysed carefully and current palletising solutions for different applications must be considered. A smart planning of packages may be further defined when the packing method is known. Restrictions in accessibility to the ULD may alter the functioning of this algorithm.

Palletising/Depalletising

The build-up of ULDs is a specialised procedure where cargo is expertly arranged onto or into a ULD. The cargo bay has 80 workstations for the build-up and breakdown of pallets. Each workstation is equipped with a platform adjustable in height made of powered rollers, as shown in Figure 1-6. Each workstation allows a ULD to be built up and to be released by the Transport Vehicle (TV) into PCHS. The platform can be lowered 1.6 meters into the ground to allow the builders to build up to a height of 3 meters. The build-up of pallets [13] is a relatively simple process. A pallet is placed on the platform and a pre-cut sheet of plastic is laid over the top. The cargo which is planned to be built up is often already present in

Figure 1-6: ULD workstation

a buffer near to the platform, and the cargo is taken from the buffer and loaded onto the pallet in whatever way the employee wants. When the cargo is on the pallet, another sheet of plastic is used to cover the cargo and the other sheet of plastic is tucked underneath the second to protect the cargo from rain and dirt when outside. The pallet is then covered with a net which will hold all the cargo in place. In case of heavy loads, extra straps will be used underneath the net to hold the cargo in place. When the sending is deemed safe to fly, it is input into PCHS from where it is processed.

Current Industrial Palletising

Industrial automated palletising is used in a variety of applications. Currently the majority of technologies used are fully automated. Three categories of fully automated palletising design may be considered [14]:

- Robot centred work cell
- In-line robot work cell
- Mobile robot work cell

The robot centred and in-line work cells both operate with a fixed in place robot, where the products move within the reach of the robot to be palletised. The mobile robot work cell contains a robot on either an overhead rail or a floor track system where the robot may change its position relative to the palletising task. For a detailed overview refer to the Literature review [15].

1-2 Problem Definition

Based on the analysis of the processes at KLM cargo and the limitation of the currently available industrial solutions, a number of design parameters may be chosen to define the problem. The palletising process needs to deal with objects of a great variety in dimensions, masses and inertial parameters. Some objects may require special handling or may be limited in their possible position on the ULD. Spacial planning of the objects position on the ULD is unknown, but may be introduced (DPPP). The physical act of palletising is currently performed by manual labour and fork lift trucks, and a full automated procedure would be extremely complicated and expensive. An ideal solution for this problem is where the heavy lifting and manual labour can be compensated by a pro-active lifting assistant, where the labourer can be free to place an object while the weight is compensated by a robotic assistant. To aid the performance and improve palletising speed, the robot may actively contribute to the motion of the object. The active contribution of a robotic assistant can be defined in the physical Human-Robot Interaction (pHRI) framework. This is a field which has grown in recent times due to the increasing interest in human and robot working together. The problem with the approaches taken by a varied number of researchers is that the object handled by the human and robot is required to be of known mass, inertial values, and dimensions. A big step in this field would be to develop such a system which would allow the robot to handle any object. Research is ongoing on this topic and currently the method used has a condition regarding persistence of excitation. A new approach has been introduced by Beyhan et al. [16] and this thesis will develop this approach for the pHRI framework.

1-3 Outline

This thesis will discuss the role of object parameters in the framework of pHRI in Chapter 2. The current approach to estimate payload parameters is an adaptive control technique which is developed in Chapter 3. The drawbacks of the traditional approach are explained, and after which an alternative approach is introduced in Chapter 4. This section will show the motivation for using the alternative approach and develop it for a two-link manipulator. Finally, the results and accompanying conclusions and recommendation will round off this thesis.

Chapter 2

Physical Human-Robot Interaction

Robots have become an everyday part of industry with their great strength, precision and constant performance as big benefactors to their success. Robots have proven their strength in repetitive and heavy tasks, but they still cannot outperform a human when it comes to dealing with a large variety of objects and problems. The process as described for Koninklijke Luchtvaart Maatschappij (KLM) is a heavy task, but also requires planning and problem solving capabilities. If an object does not quite fit where it should go, a robot would not be able to quickly find a next best solution, a robot would not nudge other objects slightly out of the way to create space for the new one. This flexibility in human thinking is what makes a human-robot team an ideal solution. The robot compensating the heavy lifting, while the human is free to deal with the placement of objects and any short term problems that come up.

The drawback of this inflexibility in robots is demonstrated in the baggage handling system at Amsterdam Airport Schiphol (SPL). The baggage handling area in Schiphol is a state of the art facility handling 70 million bags per year in a fully automated storage, sorting and transport system designed in collaboration with Vanderlande [17]. A new development in the baggage handling is the introduction of robots to load luggage for a specific destination onto a luggage cart (see Figure 2-1 [18]).

This loading process is fully automatic, but its placement of bags is not perfect and sometimes requires a person to rectify the mistakes. These small mistakes are very difficult to iron out, due to the varying nature of the suitcases and the limited capabilities of the vision system. The robot plans the placement of suitcases by a rectangular prism, which is far from a perfect representation of a suitcase. This means that when the robot thinks a spot is perfectly filled, in reality this may not be the case. This is one of the biggest drawbacks of modern day robotics and a headache for industrial processes. The proposed framework of physical Human-Robot Interaction (pHRI) is a possible solution currently in development at several institutions. One of the possible solutions close to industrial implementation is the exoskeleton developed by Daewoo [19]. This proposal (see Figure 2-2) is a passive system where the exoskeleton compensates the weight carried, but does not actively contribute to the object manipulation. This system is being tested and analysed for further development. The exoskeleton may offer

Figure 2-1: Robot sorting bags into luggage cart

Figure 2-2: Industrial exoskeleton

a great improvement in object handling as the human is now able to carry very heavy objects and manipulate them as if they were much lighter. While this Iron Man-like approach is applicable in many areas, it may be overly complicated and expensive for the application at KLM Cargo and more so, it may restrict the person in their motion due to the bulky hardware. As can be seen in Table 1-2, the size of pallets to be built up vary a lot and may require placement in tight gaps, where any wearable robot may get in the way. The sheer size of the pallet to be built also means that some objects may need to be placed in hard to reach places. For this situation it may be preferred to have a partially automated robot which could bring the object near to the area of placement where the human can adjust the object to ensure ideal placement. A collaborative approach where both the human and robot may influence the object motion offers an ideal solution for the KLM palletising problem. There are multiple institutions looking into this problem, many of which can be found in the literature review for this project [15]. One of the approaches which shows very promising results and was actively looking into the estimation of object dynamics is being investigated at the Technische Universität München (TUM) in the department Information-Oriented Control (ITR). This department has recently published a thorough overview of the cooperative manipulation task [20]. Mörtl et al. [20] clearly explains the varied aspects of the pHRI problem and uses a number of assumptions:

- 1 human with single/multiple robots,
- Constraints of the environment are such that the task is achievable,
- Rigid object is tightly grasped and of known shape and dynamics,
- Object dynamics are holonomic,
- Grasp points are such that the task is controllable and its control inputs are redundant [21],
- Haptic communication only through physical coupling.

These assumptions create the basis for the task of a robot and human transporting a rigid body of known dynamics to a commonly known location. For the application at KLM, the object dynamics may not be known, and in order for this information to be determined, a parameter estimation scheme can be utilized. In order to implement such a scheme, it is important to understand how the cooperative scheme works. According to Salleh et al. [22] an object centred formulation of the problem results in the smoothest transfer of the object. This means that the problem will be approached as shown in Figure 2-3 where the object is described in Eq. (2-1).

$$\mathbf{M}_c\ddot{\mathbf{x}}_c + \mathbf{f}_c(\mathbf{x}_c, \dot{\mathbf{x}}_c) = \mathbf{u}_c \tag{2-1}$$

Where $\mathbf{x}_c$ is the configuration of an object of inertia $\mathbf{M}_c$ with external wrench $\mathbf{u}_c$ and environmental forces $\mathbf{f}_c$. In the cooperative robotics scheme the payload dynamics fits into the inverse dynamics section as shown in Figure 2-4. The information required by this system to function consists of the mass and its inertia matrix. The object dynamics are estimated in this paper using an off-line estimation procedure prior to any experimentation. This limitation can be surpassed by using an on-line estimation procedure to determine the object dynamic properties. Current research at the TUM is focussed on the analysis of the objects'

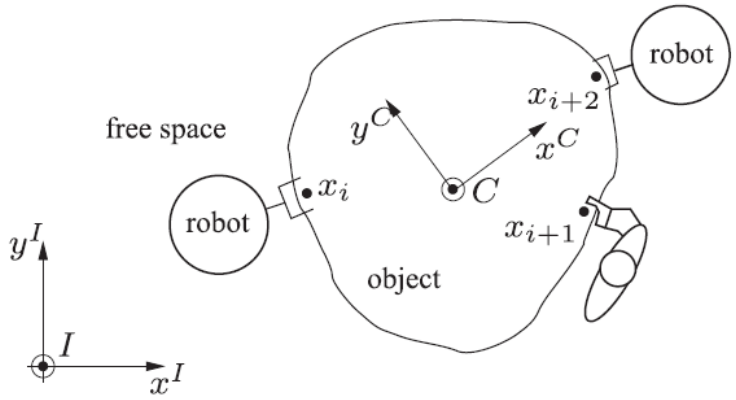

Figure 2-3: Object centred model

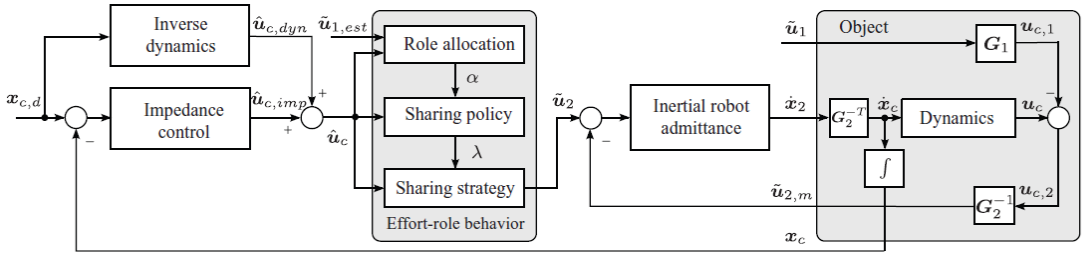

Figure 2-4: Object centred model

properties using a traditional adaptive control strategy. This strategy has been proven to be effective and the control algorithm shows good results for estimation and trajectory tracking [23]. This strategy will be described in the next chapter.

Chapter 3

Composite Adaptive Control

An approach to estimate the object parameters, currently under development at TUM, is an adaptive control scheme originally developed by Slotine and Li [24]. Three adaptive control approaches are shown in a report by Vijverstra [23], the direct, indirect and composite adaptive control approaches. Vijverstra showed that the best performance overall was given by the composite approach which can be used in the framework for physical Human-Robot Interaction (pHRI). The approach is developed in this chapter and will be tested for a two-link manipulator. The results will offer a basis for comparison to an alternative approach shown in in Chapter 4.

3-1 Composite Adaptive Control

A rigid body manipulator may be defined as Eq. (3-1).

$$H(q(t))\ddot{q}(t) + C(q(t), \dot{q}(t))\dot{q}(t) + G(q(t)) = \tau(t) \tag{3-1}$$

where,

- $H(q(t))$ is a symmetric positive definite manipulator inertia matrix,
- $C(q(t), \dot{q}(t))$ is a matrix of centripetal and coriolis torques,
- $G(q(t))$ is a vector with gravitational torques,
- $q(t)$ is a vector of generalized coordinates,
- $\dot{q}(t)$ is a vector of generalized velocities,

- $\ddot{q}(t)$ is a vector of generalized accelerations,

- $\tau(t)$ is a vector of torque inputs.

The dynamics described are linear in terms of well selected parameters, known as the linear parametrization property. Therefore, the robot dynamics can be rewritten as in Eq. (3-2), where $a(t)$ is a vector with payload and robot parameters, and $Y(q(t), \dot{q}(t), \ddot{q}(t))$ is a nonlinear matrix function. The payload is the object handled by the robot.

$$Y(q(t), \dot{q}(t), \ddot{q}(t))a(t) = \tau(t) \tag{3-2}$$

Within this framework, the following tracking parameters may be defined:

- $q_d(t)$ is the desired trajectory of the generalized coordinates,
- $\dot{q}_d(t)$ is the desired trajectory of the generalized velocities,
- $\ddot{q}_d(t)$ is the desired trajectory of the generalized accelerations.

The control purpose is to derive a control law for $\tau(t)$ which drives $q(t), \dot{q}(t), \ddot{q}(t)$ to $q_d(t), \dot{q}_d(t), \ddot{q}_d(t)$, and an adaptation law for the unknown parameters $a(t)$. The tracking error for such a system is defined by $\varepsilon_t(t)$ in Eq. (3-3).

$$\varepsilon_t(t) = \dot{\tilde{q}}(t) + \Lambda\tilde{q}(t) \tag{3-3}$$

where,

- Λ is a constant positive definite matrix,

- $\tilde{q}(t) = q(t) - q_d(t)$ is the difference between the desired and true states.

The adaptive controllers were designed by letting the estimated parameters $\hat{a}(t)$ be used in the system matrices such that the control law may be written as shown in Eq. (3-4).

$$\begin{aligned} \hat{H}(q(t))\ddot{q}(t) + \hat{C}(q(t), \dot{q}(t))\dot{q}(t) + \hat{G}(q(t)) - K_D\varepsilon_t(t) &= \tau(t) \\ Y(q(t), \dot{q}(t), \dot{q}_r(t), \ddot{q}_r(t))\hat{a}(t) - K_D\varepsilon_t(t) &= \tau(t) \end{aligned} \tag{3-4}$$

where,

- $\hat{H}(q(t))$ is a symmetric positive definite manipulator inertia matrix,

- $\hat{C}(q(t), \dot{q}(t))$ is a matrix of centripetal and coriolis torques,

- $\hat{G}(q(t))$ is a vector with gravitational torques,

- $\dot{q}_r(t)$ is the reference velocity, $\dot{q}_r(t) = \dot{q}_d(t) - \Lambda\tilde{q}(t)$,

- $\ddot{q}_r(t)$ is the reference acceleration, $\ddot{q}_r(t) = \ddot{q}_d(t) - \Lambda\dot{\tilde{q}}(t)$,

- K_D is a Constant positive definite matrix to regulate the tracking error.

Slotine and li [24] have analysed the issues of parameter convergence and shown that this is dependent on a persistence of excitation condition. The adaptation law for a composite adaptive control system is given in Eq. (3-5).

$$\begin{aligned} \text{Adaptation Law :} \quad & \dot{\hat{a}}(t) = -P(t)\left[Y(q(t),\dot{q}(t),\ddot{q}(t))^T\varepsilon_t(t) + Y^T(q(t),\dot{q}(t),\ddot{q}(t))R(t)e(t)\right] \\ \text{Adaptation Gain :} \quad & \dot{P}(t) = \lambda(t)P(t) - P(t)Y^T(q(t),\dot{q}(t),\ddot{q}(t))Y(q(t),\dot{q}(t),\ddot{q}(t))P(t) \\ \text{Forgetting Rate :} \quad & \lambda(t) = \lambda_0\left(1 - \frac{\|P(t)\|}{k_0}\right) \end{aligned} \tag{3-5}$$

where,

- $e(t)$ is the prediction error $\hat{y}(t) - y(t)$,

- $P(t)$ is the Time-varying positive definite gain matrix,

- $R(t)$ is a uniformly positive definite weighting matrix indicating how much attention should be payed to the parameter information in the prediction error,

- $\lambda(t)$ is the forgetting factor,

- λ_0 is the maximum forgetting rate,

- k_0 is the upper bound of the gain matrix norm.

Vijverstra [23] demonstrates the global tracking convergence of the composite control through Lyapunov analysis. The conditions include bounded desired trajectories and persistence of excitation, which results in tracking and prediction errors being globally exponentially convergent.

3-2 Example: Two-link manipulator

To demonstrate the abilities of the composite adaptive controller and to test the conditions of persistence of excitation, a two-link manipulator will be considered as shown in Figure 3-1. This manipulator will be considered without gravitational and inertial influences for simplicity.

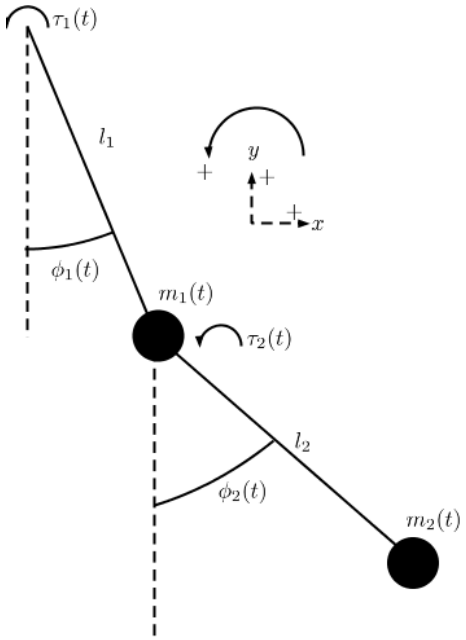

Figure 3-1: The two-link manipulator

3-2-1 Plant

The model plant will be described in its generalized states $q(t) = [\phi_1(t), \phi_2(t)]^T$, where $\phi_1(t)$ and $\phi_2(t)$ are as shown in Figure 3-1. The system matrices may therefore be described by Eq. (3-6).

$$\begin{aligned} H(q(t)) &= \begin{bmatrix} (m_1(t)+m_2(t))l_1^2 & m_2(t)l_1l_2\cos(\phi_1(t)-\phi_2(t)) \\ m_2(t)l_1l_2\cos(\phi_1(t)-\phi_2(t)) & m_1(t)l_2^2 \end{bmatrix} \\ C(q(t),\dot{q}(t)) &= \begin{bmatrix} 0 & m_2(t)l_1l_2\dot{\phi}_2(t)\sin(\phi_1(t)-\phi_2(t)) \\ m_2(t)l_1l_2\dot{\phi}_1(t)\sin(\phi_1(t)-\phi_2(t)) & 0 \end{bmatrix} \\ G(q(t)) &= 0 \end{aligned} \tag{3-6}$$

where,

- l_1 is the length of first manipulator link,
- l_2 is the length of second manipulator link,
- m_1 is the mass at the end of the first link,
- m_2 is the mass at the end of the second link.

To rearrange this representation into Eq. (3-2), the mass and length parameters in $H(q(t))$ and $C(q(t), \dot{q}(t))$ may be replaced by terms in the parameter vector $a(t) = [a_1(t), a_2(t), a_3(t)]^T$ as shown in Eq. (3-7).

$$H(q(t)) = \begin{bmatrix} a_1(t) & a_2(t)\cos(\phi_1(t) - \phi_2(t)) \\ a_2(t)\cos(\phi_1(t) - \phi_2(t)) & a_3 \end{bmatrix}$$
$$C(q(t), \dot{q}(t)) = \begin{bmatrix} 0 & a_2(t)\dot{\phi}_2(t)\sin(\phi_1(t) - \phi_2(t)) \\ a_2(t)\dot{\phi}_1(t)\sin(\phi_1(t) - \phi_2(t)) & 0 \end{bmatrix}$$

where,

$$a = \begin{bmatrix} (m_1(t) + m_2(t))l_1^2 \\ m_2(t)l_1l_2 \\ m_1(t)l_2^2 \end{bmatrix}$$

The system above may be written in the linear parametrization form as shown in Eq. (3-7).

$$Y(q(t), \dot{q}(t), \ddot{q}(t)) = \begin{bmatrix} \ddot{\phi}_1(t) & \cos(\phi_1(t) - \phi_2(t))\ddot{\phi}_2(t) + \sin(\phi_1(t) - \phi_2(t))\dot{\phi}_2^2(t) & 0 \\ 0 & \cos(\phi_1(t) - \phi_2(t))\ddot{\phi}_1(t) - \sin(\phi_1(t) - \phi_2(t))\dot{\phi}_1^2(t) & \ddot{\phi}_2(t) \end{bmatrix} \tag{3-7}$$

To write this function in the form as shown in Eq. (3-4), the reference parameters must be introduced to generate the function in Eq. (3-8).

$$Y(q(t), \dot{q}(t), \dot{q}_r(t), \ddot{q}_r(t)) = \begin{bmatrix} \ddot{\phi}_{1r}(t) & \cos(\phi_1(t) - \phi_2(t))\ddot{\phi}_{2r}(t) + \sin(\phi_1(t) - \phi_2(t))\dot{\phi}_2(t)\dot{\phi}_{2r}(t) & 0 \\ 0 & \cos(\phi_1(t) - \phi_2(t))\ddot{\phi}_{1r}(t) - \sin(\phi_1(t) - \phi_2(t))\dot{\phi}_1(t)\dot{\phi}_{1r}(t) & \ddot{\phi}_{2r}(t) \end{bmatrix} \tag{3-8}$$

3-2-2 Desired Trajectory

The desired trajectory will be a step-wise reference between $\pi/4$ and 0 every five seconds for $\phi_1(t)$ and 2.5 seconds for $\phi_2(t)$ as shown in Figure 3-2. Using a step-wise reference means that the derivatives of the desired trajectories are 0. These reference signals are used to demonstrate the response with persistence of excitation. The reference signal without persistence of excitation will be demonstrated by a simple step towards $\pi/4$ for both link angles.

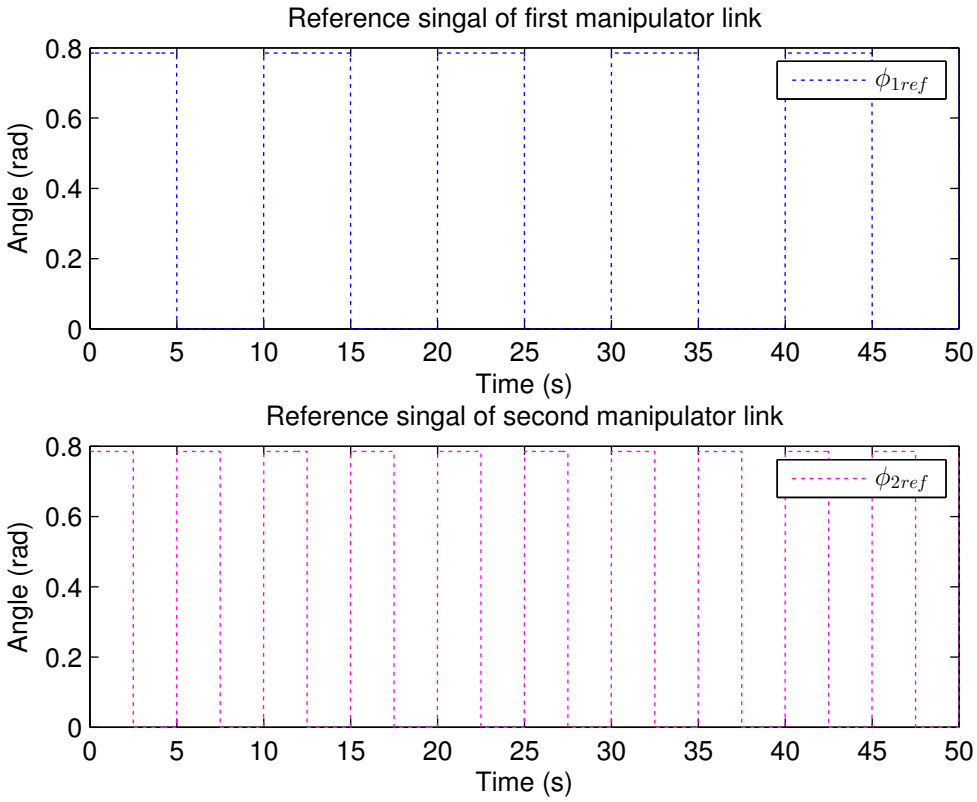

Figure 3-2: Reference signal with persistence of excitation

3-2-3 System Parameters

The initial conditions of the system and its control parameters are shown below.

$$
\begin{aligned}
m_1(t) &= 2\text{kg} \\
m_2(t) &= 3\text{kg} \\
l_1 &= 2\text{m} \\
l_2 &= 3\text{m} \\
a_1 &= 5 \\
a_2 &= 3 \\
a_3 &= 3 \\
\hat{a}_1(0) &= 0\text{kg} \\
\hat{a}_2(0) &= 0\text{kg} \\
\hat{a}_3(0) &= 0\text{kg} \\
K_D &= 700 I_{2\times 2} \\
\Lambda &= I_{2\times 2} \\
P(0) &= I_{3\times 3} \\
R(t) &= I_{3\times 3} \\
\lambda_0 &= 1 \\
k_0 &= 1
\end{aligned}
$$

3-2-4 Results

The results shown consist of two parts. The first part will show the tracking and estimation response of the system under persistence of excitation, whereas the second will demonstrate the response when the desired trajectory is not fulfilling the persistence of excitation condition.

Persistence of excitation condition fulfilled

When the desired trajectory is a step-wise reference, the estimation of the mass parameters converges to the true levels as can be seen in Figure 3-4. The tracking response of the system also converges to the desired level as can be seen in Figure 3-3.

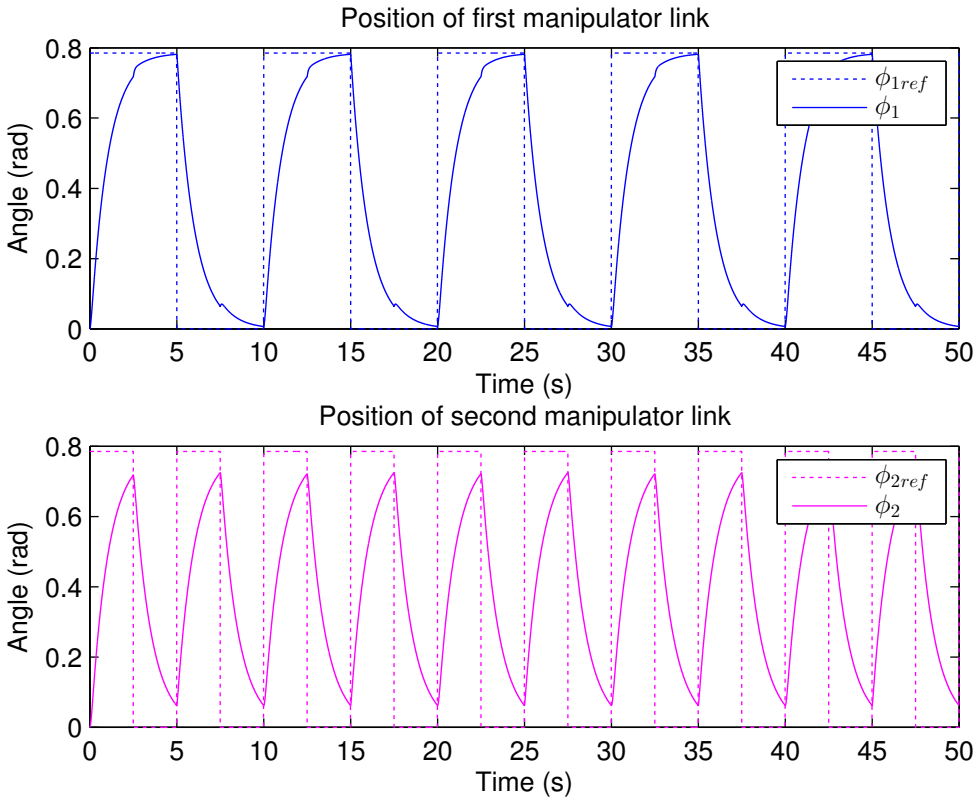

Figure 3-3: Tracking response

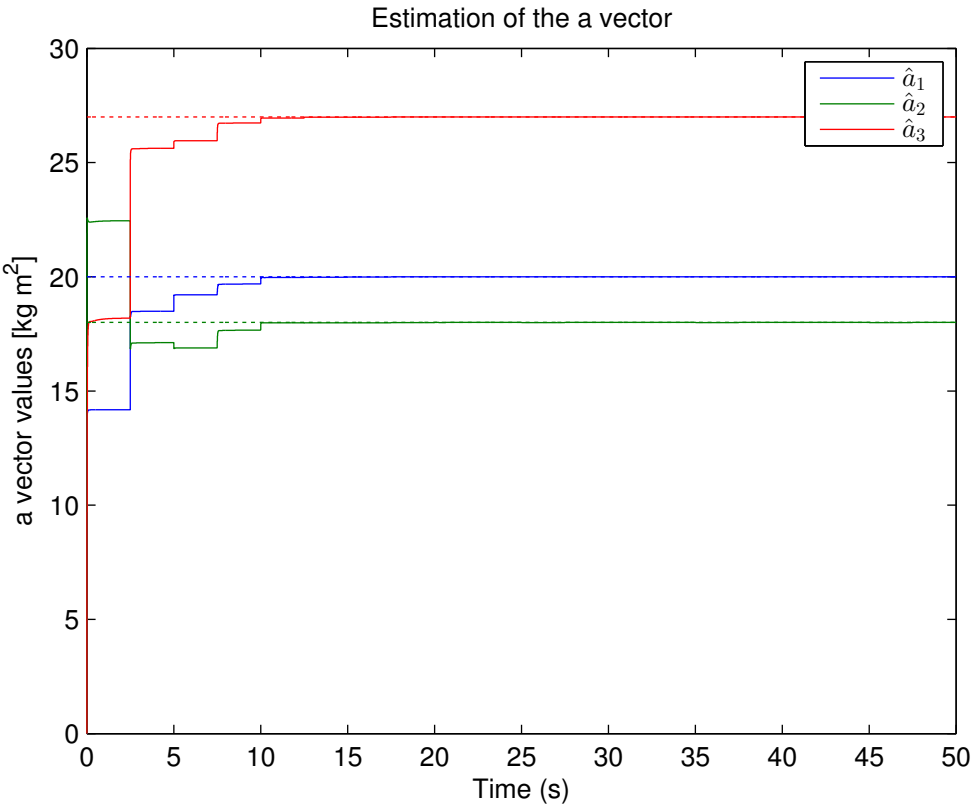

Figure 3-4: Estimation response

Persistence of excitation condition not fulfilled

When the desired trajectory is a step signal, the estimation of the mass parameters does not converge to the true levels as can be seen in Figure 3-6. The tracking response of the system does converge to the desired level as can be seen in Figure 3-5.

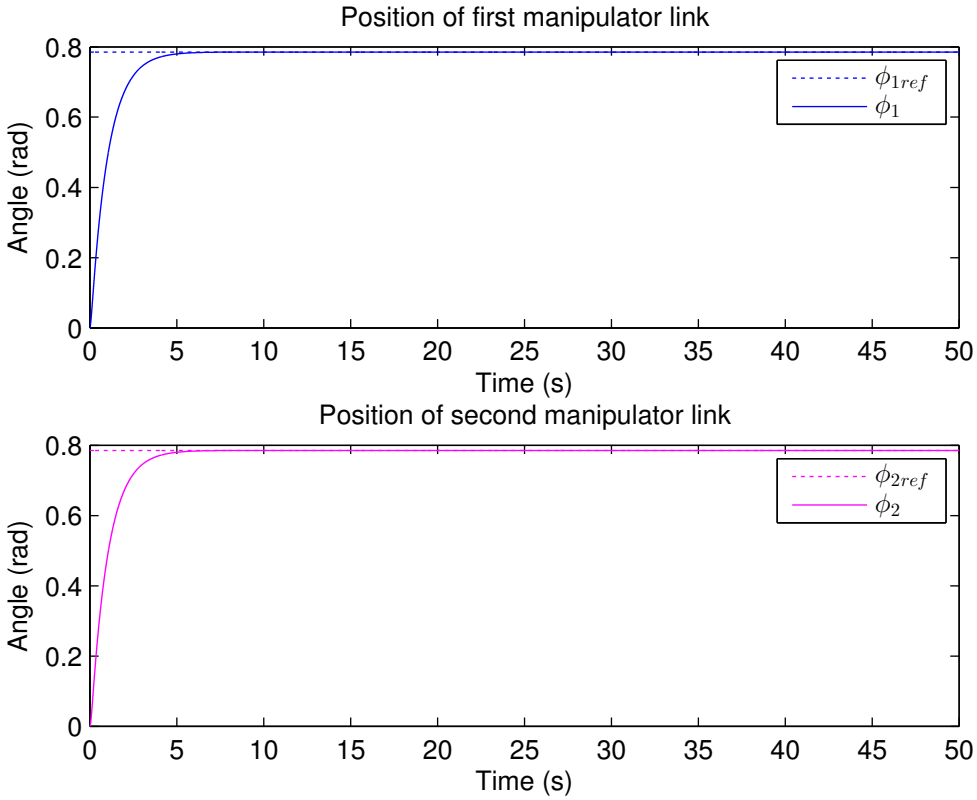

Figure 3-5: Tracking response

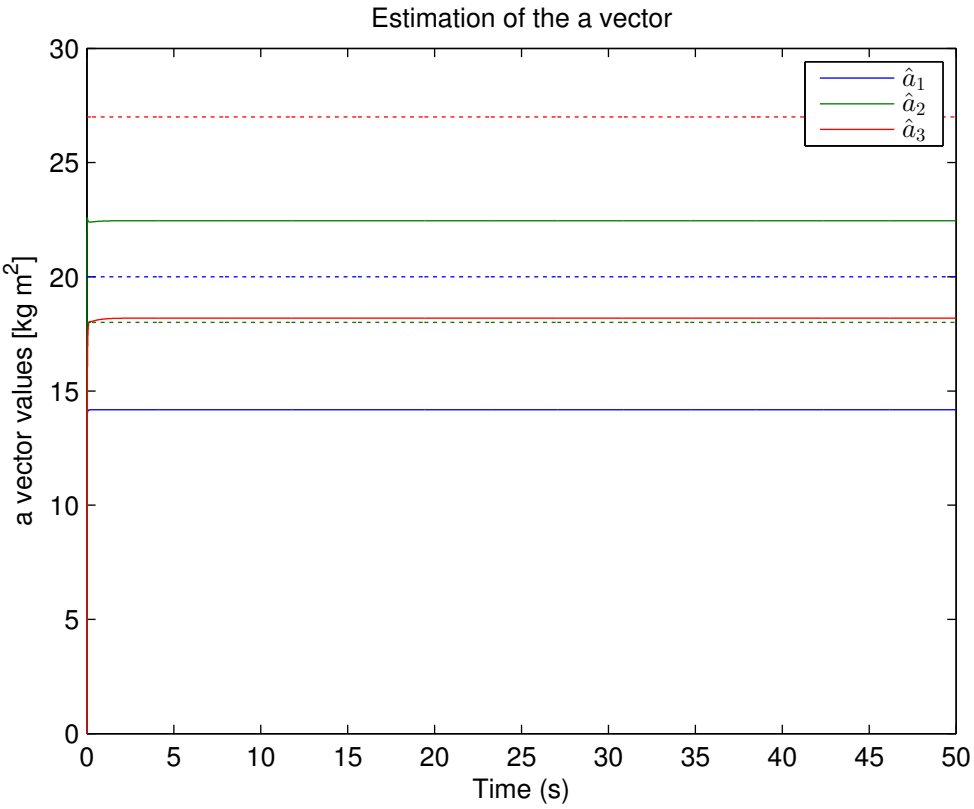

Figure 3-6: Estimation of the a vector

3-2-5 Discussion

The simulations above show that for a signal which is persistently exciting, the estimation of the mass parameters converges very quickly. The $\hat{a}(t)$ values rise to the correct figures within 12 seconds, which may be improved through other continuously exciting signal or increasing the adaptation rate by introducing a new tuning parameter k_1 into the adaptation law as shown in Eq. (3-9).

$$\dot{\hat{a}}(t) = -k_1 P(t) \left[Y^T(q(t), \dot{q}(t), \ddot{q}(t)) \varepsilon_t(t) + Y^T(q(t), \dot{q}(t), \ddot{q}(t)) R(t) e(t) \right] \tag{3-9}$$

This may improve the speed of convergence but that is not the focus of this thesis. As can be seen in the second simulation, a single impulse for the angles will not provide enough information to achieve convergence at the correct values. This means that when a two-link manipulator attempts to achieve a task with an object of unknown mass, it must follow a specific trajectory to find the correct estimate. This will require time and a potentially erratic motion by the robot. Since the robot is to function in the vicinity of humans, such a motion is not desirable. A recent development in fuzzy observer design has shown that there is an alternative to this approach. This will be discussed in the next chapter.

Chapter 4

Fuzzy Adaptive Control

To introduce the alternative method for estimating masses of a two-link manipulator, first an introduction to fuzzy logic will be given. The alternative method, as shown by Beyhan et al. [16], consists of rewriting the nonlinear model into a fuzzy approximation and using an observer to estimate the states. This paper will be explained after the introduction to fuzzy logic, after which the approach will be developed for the two-link manipulator. Two types of observers will be considered and simulation results will be shown.

4-1 Fuzzy Systems

4-1-1 Fuzzy sets

A fuzzy set is a method for defining sets which may not be optimal for use with classical sets. These sets may often consist of vague concepts such as tall, short, big, small, hot, cold, and many more. While classical sets determine an element to either belong to that set or not, a fuzzy set may gradually assess the membership. An example of the effectiveness of describing concepts such as height as a fuzzy set can be shown by considering the following statement:

"John is tall".

This statement may be analysed with classical sets by defining measures of height in a set of tall men, M, and its membership, $\mu_M(x)$ as shown in Eq. (4-1).

$$\mu_M(h) = \begin{cases} 1 & \text{if } h \geq 180\ cm \\ 0 & \text{if } h < 180\ cm \end{cases} \tag{4-1}$$

Therefore, if John has a height of 179.5 cm, he may be defined as short ($\mu_M(179.5) = 0$) but if he is 180 cm, he is tall ($\mu_M(180) = 1$). Intuition says that a difference of 0.5 cm should not make the difference between being labelled tall or short. Defining height as a fuzzy set can

solve this. We may define the fuzzy set of height as shown in Eq. (4-2). The set is shown in Figure 4-1.

$$\mu_M(h) = \begin{cases} 1 & \text{if } h \geq 190\ cm \\ (0,1) & \text{if } 170\ cm < h < 190\ cm \\ 0 & \text{if } h \leq 170\ cm \end{cases} \tag{4-2}$$

This method of using membership functions to represent sets is applicable to a large range

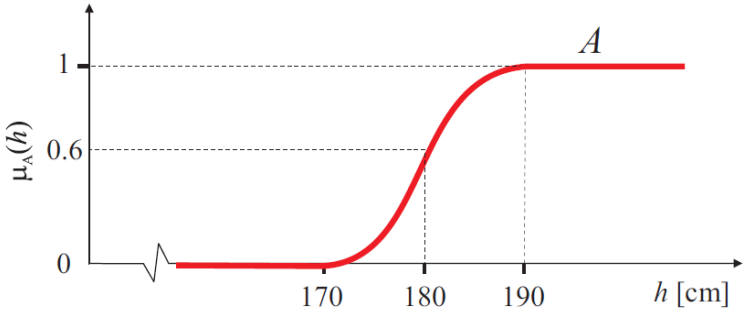

Figure 4-1: Fuzzy description of height

of topics. The membership function may take many shapes as shown in Figure 4-2. These membership functions can be used to build fuzzy models.

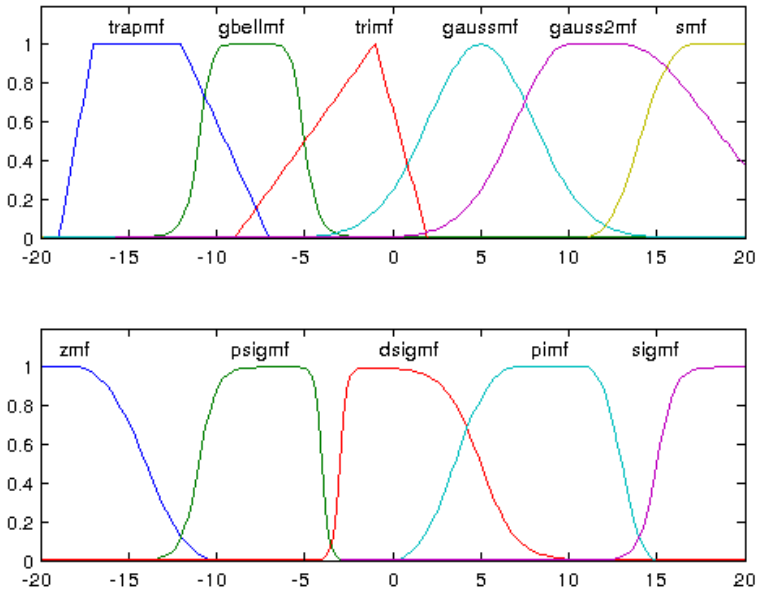

Figure 4-2: Membership functions

4-1-2 Fuzzy models

A fuzzy model may be used for imitating processes which are difficult to model with classical mathematics. One of the main strengths is that fuzzy models have the power to imitate nonlinear systems through a number of linear systems at specific operating points as explained by Lendek et al. [25] . The Takagi-Sugeno (TS) fuzzy model is one approach developed by Takagi and sugeno [26]. This approach consists of *if-then* rules as shown in Eq. (4-3).
R^i : If z_1 is Z_1^i and $\cdots$ and z_p is Z_p^i then

$$\mathbf{y} = f_i(\mathbf{z}), \qquad i = 1, 2, \ldots, m \tag{4-3}$$

where,

- R^i is the i-th model rule for a total of m rules,
- z_p is a vector of p antecedent variables,
- Z_p^i are the antecedent fuzzy sets,
- $\mathbf{y}$ is the model output,
- $f_i(\mathbf{z})$ is the consequent vector function often dependent on the scheduling variables.
- $\mathbf{z}$ is the vector of scheduling variables.

This rule based system may be described as shown in Figure 4-3[1]. Each of the three sections

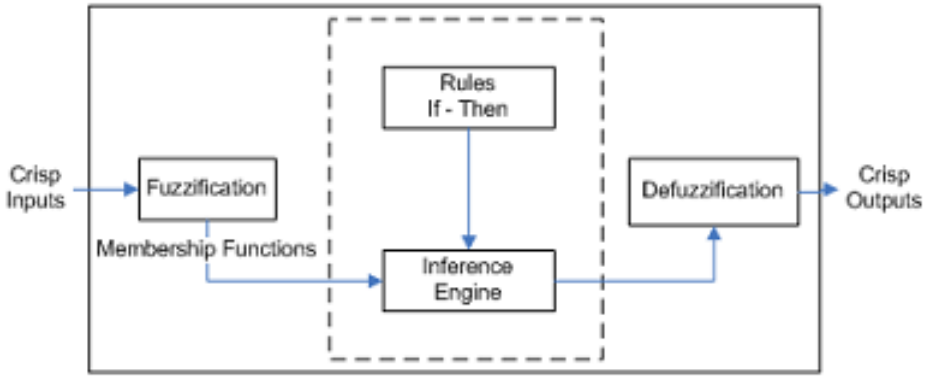

Figure 4-3: Fuzzy inference

in this figure corresponds to parts of the fuzzy model. The fuzzification occurs in the mapping of z_p onto Z_p^i after which the fuzzy inference engine utilizes the *if-then* rules to compute the output fuzzy variables. These are then defuzzified by computing the weighted combination of the output of the rules. The fuzzification produces a certain truth value given by a membership function $\omega_{ij} : \mathbb{R} \to [0, 1]$. The truth value $\varphi_i(\mathbf{z})$ for an entire rule is found based on the premise variables using a conjunction operator such as the algebraic product as shown in Eq. (4-4).

$$\varphi_i(\mathbf{z}) = \prod_{j=1}^{p} \omega_{ij}(z_j) \tag{4-4}$$

[1] http://www.tribalengineering.com/technology/fuzzy-ictl.aspx

The obtained truth value is normalized using Eq. (4-5).

$$w_i(\mathbf{z}) = \frac{\varphi_i(\mathbf{z})}{\sum_{j=1}^{m} \varphi_i(\mathbf{z})} \tag{4-5}$$

Where $w_i(\mathbf{z})$ is the normalized membership function. In this normalization it is assumed that $\sum_{j=1}^{m} \varphi_i(\mathbf{z}) \neq 0$. The output of rule i is then defuzzified using the normalized membership function to compute the weighted combination of the output of the rules as shown in Eq. (4-6).

$$\mathbf{y} = \sum_{i=1}^{m} w_i(\mathbf{z}) f_i(\mathbf{z}) \tag{4-6}$$

This approach may be used to represent or approximate a nonlinear function by choosing the consequent functions as linear or affine functions. These functions will be called local functions as they are only valid locally, i.e., where the value of the corresponding normalized membership function is zero. The final outputs of the TS fuzzy models are computed as shown in Eq. (4-7).

$$\begin{aligned} \dot{\mathbf{x}} &= \sum_{i=1}^{m} w_i(\mathbf{z})(A_i\mathbf{x} + B_i\mathbf{u}) \\ \mathbf{y} &= \sum_{i=1}^{m} w_i(\mathbf{z})(C_i\mathbf{x}) \end{aligned} \tag{4-7}$$

where,

- A_i is the i-th state matrix,
- B_i is the i-th input matrix,
- C_i is the i-th output matrix,
- $\mathbf{x}$ is the state vector of the system,
- $\dot{\mathbf{x}}$ is the derivative of the state vector of the system.

4-2 Sector Nonlinearity Approach

TS Fuzzy Model

The sector nonlinearity approach, first described by Ohtake et al. [27], is a method for constructing TS fuzzy models. Lendek et al. [25] show that for a nonlinear system of equations given by the form as shown in Eq. (4-8), the sector nonlinearity approach may be applied.

$$\begin{aligned} \dot{\mathbf{x}} &= f(\mathbf{x}, \mathbf{u})\,\mathbf{x} + g(\mathbf{x}, \mathbf{u})\,\mathbf{u} \\ \mathbf{y} &= h(\mathbf{x}, \mathbf{u})\,\mathbf{x} \end{aligned} \tag{4-8}$$

where,

- $f(\mathbf{x}, \mathbf{u})$, $g(\mathbf{x}, \mathbf{u})$, $h(\mathbf{x}, \mathbf{u})$ are nonlinear matrix functions,

- $\mathbf{x} \in \mathbb{R}^{n_x}$ is the state vector,
- $\mathbf{u} \in \mathbb{R}^{n_u}$ is the input vector,
- $\mathbf{y} \in \mathbb{R}^{n_y}$ is the output vector.

The sector nonlinearity approach allows the construction of a fuzzy system given a number of assumptions:

- All variables are assumed to be defined on a compact set,
- $f(\mathbf{x}, \mathbf{u})$, $g(\mathbf{x}, \mathbf{u})$, $h(\mathbf{x}, \mathbf{u})$ are smooth functions with bounded elements.

Scheduling variables may be chosen as $z_j(\cdot) \in [\underline{nl}_j, \overline{nl}_j], j = 1, 2, \cdots, p$ where each z_j variable represents a non-constant term in f, g and h, and $\underline{nl}_j$ and $\overline{nl}_j$ are the minimum and maximum, respectively, of z_j. For each z_j, two weighting functions, $\eta_0^j(\cdot)$ and $\eta_1^j(\cdot)$ can be constructed as shown in Eq. (4-9).

$$\eta_0^j(\cdot) = \frac{\overline{nl}_j - z_j(\cdot)}{\overline{nl}_j - \underline{nl}_j} \qquad \eta_1^j(\cdot) = 1 - \eta_0^j(\cdot) \qquad j = 1, 2, \cdots, p \tag{4-9}$$

The following properties are true for these weighting functions.

- $\eta_0^j(\cdot) \geq 0$,
- $\eta_1^j(\cdot) \geq 0$,
- $\eta_0^j(\cdot) + \eta_1^j(\cdot) = 1$,
- $z_j = \underline{nl}_j \eta_0^j(z_j) + \overline{nl}_j \eta_1^j(z_j)$.

The product of the weighting functions that correspond to the fuzzy sets in the rule computes the membership function $w_i(\mathbf{z})$ of rule i.

$$w_i(\mathbf{z}) = \prod_{j=1}^{p} \eta_{0,1}^j(z_j) \tag{4-10}$$

where,

- $\eta_{0,1}^j(z_j)$ is either $\eta_0^j(z_j)$ or $\eta_1^j(z_j)$ depending on whether the weighting function used in the rule is the minimum or maximum respectively,
- $w_i(\mathbf{z}) \geq 0$,
- $\sum_{i=1}^{m} w_i(\mathbf{z}) = 1$.

The matrices A_i, B_i, and C are constructed by substituting the maximum and minimum values of the scheduling variables into their corresponding position within the original matrix and vector functions f, g, and h. Then, using the membership functions defined by Eq. (4-10), the original nonlinear system (Eq. (4-8)) is exactly represented by the TS fuzzy model shown in Eq. (4-11).

$$\begin{aligned} \dot{\mathbf{x}} &= \sum_{i=1}^{m} w_i(\mathbf{z}_j)\,(A_i\mathbf{x} + B_i\mathbf{u}) \\ \mathbf{y} &= \sum_{i=1}^{m} w_i(\mathbf{z}_j)\,(C_i\mathbf{x}) \end{aligned} \tag{4-11}$$

For the problem at hand, the TS fuzzy model can be simplified by assuming the output signals are the same for each rule. This means the new TS fuzzy model will be defined as shown in Eq. (4-12).

$$\begin{aligned} \dot{\mathbf{x}} &= \sum_{i=1}^{m} w_i(\mathbf{z}_j)\,(A_i\mathbf{x} + B_i\mathbf{u}) \\ \mathbf{y} &= C\mathbf{x} \end{aligned} \tag{4-12}$$

4-3 Adaptive fuzzy payload estimation

A recent publication by Beyhan et al. [16] uses the TS fuzzy model to create an extended state vector $\mathbf{x}$. The approach taken by this paper is to use the sector nonlinearity approach to find the fuzzy approximation of a nonlinear Single-Input Single-Output (SISO) system. The nonlinear system discussed in this paper is a robot manipulator shown in Figure 4-4. This

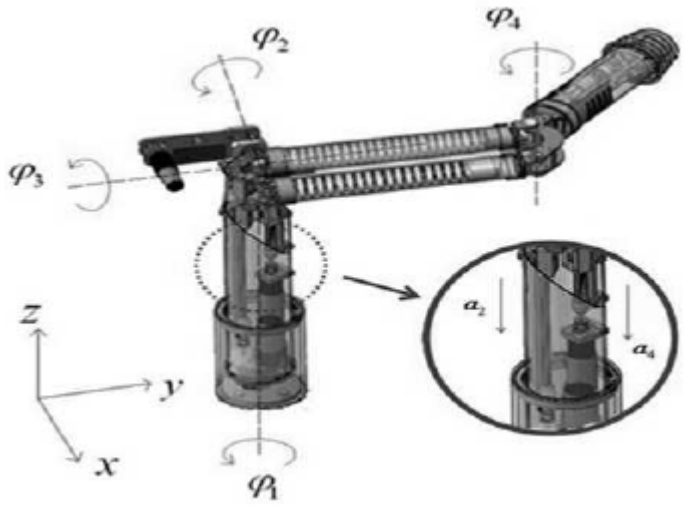

Figure 4-4: Robot arm

robot arm may be described by the general dynamics as shown in Eq. (4-13).

$$\begin{aligned} mL^2\ddot{\varphi}(t) + (Kdr - mgl)\sin(\varphi(t)) &= \tau(t) \\ Kd - Kr\cos(\varphi(t)) &= F(t) \end{aligned} \tag{4-13}$$

where,

- $\varphi(t)$ is the angle of the robot arm,
- $\ddot{\varphi}(t)$ is the angular acceleration of the robot arm,
- $\tau(t)$ is the driving torque,
- $F(t)$ is the driving force,
- d is the vertical projection of the spring displacement,
- m is the payload mass,
- L= 0.4m is the length of the link,
- r= 0.075m is the length of the spring arm,
- K= 568Nm is the spring constant,
- g= 9.81ms² is the acceleration due to gravity.

Each of the variables described above are shown in Figure 4-5. To simplify this system to a SISO representation, the driving torque will be set to $\tau(t) = 0$. As the payload mass will be assumed non-constant, the m parameter will be considered as $m(t)$. With a change of variables where $x_1(t) = \varphi(t)$ and $x_2(t) = \dot{\varphi}(t)$ the system may be written as shown in Eq. (4-14). For simplicity $x_1(t)$, $x_2(t)$, and $\mathbf{y}(t)$ will be written as x_1, x_2, and $\mathbf{y}$ respectively.

$$\begin{aligned} \dot{x}_1 &= x_2 \\ \dot{x}_2 &= \sin(x_1)\frac{g}{L} - \frac{r\sin(x_1)(Kr\cos(x_1) + F(t))}{L^2 m(t)} \\ \mathbf{y} &= x_1 \end{aligned} \tag{4-14}$$

The mass parameter ($m(t)$) in this representation consists of two parts, a payload to be carried ($m_L(t)$) and the mass of the end-effector (m_e). The maximum and minimum values for the parameters are:

- $F(t) \in [0, 160]$ N
- $x_1 \in [\frac{\pi}{2}, \pi]$ rad
- $m(t) \in [0.35, 2]$ kg where $m_e = 0.35$ kg

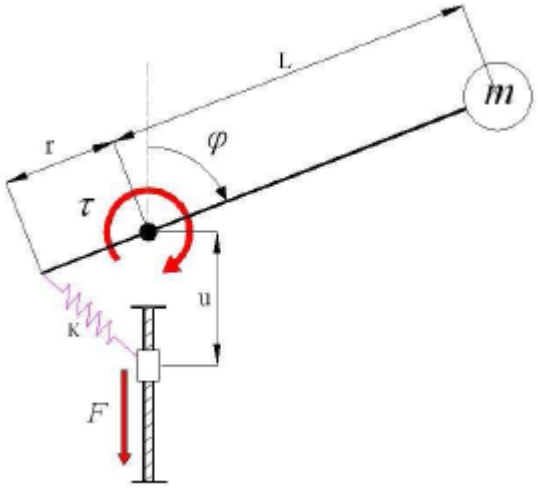

Figure 4-5: A schematic representation of the arm

The varying payload parameter is unknown and needs to be estimated. To do so, an extra state may be added to Eq. (4-14) containing the mass parameters as shown in Eq. (4-15).

$$x_3(t) = x_3 = \frac{m_L(t)}{m_e + m_L(t)} \tag{4-15}$$

This means that the extended nonlinear system may be written as shown in Eq. (4-16). Since $m_L(t)$ is a piecewise constant variable, x_3 inherits that property. Therefore, $\dot{x}_3$ becomes equal to zero except for a set of Lebesgue measure zero.

$$\begin{aligned} \dot{x}_1 &= x_2 \\ \dot{x}_2 &= \sin(x_1)\frac{g}{L} - \frac{r\sin(x_1)(Kr\cos(x_1) + F(t))}{m_e L^2)}(1 - x_3) \\ \dot{x}_3 &= 0 \\ \mathbf{y} &= x_1 \end{aligned} \tag{4-16}$$

4-3-1 Sector nonlinearity approach applied

Eq. (4-16) may be transformed into a TS fuzzy system through the sector nonlinearity approach, into a slightly different form than the one shown in Eq. (4-11). An alternative to this is to introduce the form where affine terms are added to the system in the form of $a_i(\mathbf{y})$. A fuzzy scheduling variable is introduced as defined in Eq. (4-17).

$$\mathbf{z} = \frac{r\sin(x_1)(Kr\cos(x_1) + F(t))}{m_e L^2)} \in [16.76, 214.28] \tag{4-17}$$

Therefore, the TS fuzzy model may be defined as shown in Eq. (4-18), where C_i is independent of the scheduling variable.

$$\begin{aligned} \dot{\mathbf{x}} &= \sum_{i=1}^{m} w_i(\mathbf{z}_j)\left(A_i\mathbf{x} + a_i(\mathbf{y})\right) \\ \mathbf{y} &= C_i\mathbf{x} \end{aligned} \tag{4-18}$$

Where the weighting functions and local matrices become:

$$w_1(\mathbf{z}) = \frac{214.28 - \mathbf{z}}{214.28 - 16.76}, \qquad w_2(\mathbf{z}) = 1 - w_1(\mathbf{z})$$

$$A_1 = \begin{bmatrix} 0 & 1 & 0 \\ 0 & 0 & 16.76 \\ 0 & 0 & 0 \end{bmatrix}, \qquad A_1 = \begin{bmatrix} 0 & 1 & 0 \\ 0 & 0 & 214.28 \\ 0 & 0 & 0 \end{bmatrix}$$
$$a_1 = \begin{bmatrix} 0 \\ \sin(\mathbf{y})\frac{g}{L} - 16.76 \end{bmatrix}, \qquad a_2 = \begin{bmatrix} 0 \\ \sin(\mathbf{y})\frac{g}{L} - 214.28 \end{bmatrix}$$
$$C = \begin{bmatrix} 1 & 0 & 0 \end{bmatrix}$$

4-3-2 Observer design

Regarding the observer design for TS fuzzy systems, there are two approaches. The firsts requires a scheduling variable consisting entirely of measured states, and the second where the scheduling variable contains unmeasured states. For the example given by Beyhan et al., the only state required for the calculation of $\mathbf{z}$ is x_1. Therefore, the first approach may be used. An observer of this description is the fuzzy Luenberger observer [28] [29]. This observer is a generalisation of the classical Luenberger observer to fuzzy systems, hereafter referred to as the fuzzy observer. An observer of this kind is described by Eq. (4-19).

$$\begin{aligned} \dot{\hat{\mathbf{x}}} &= \sum_{i=1}^{m} w_i(\mathbf{z}) \left(A_i \hat{\mathbf{x}} + a_i(\mathbf{y}) + L_i(\mathbf{y} - \hat{\mathbf{y}}) \right) \\ \hat{\mathbf{y}} &= C\hat{\mathbf{x}} \end{aligned} \tag{4-19}$$

where L_i are the observer gains, $\hat{\mathbf{y}}$ are the estimated model outputs, $\hat{\mathbf{x}}$ are the estimated model states and $\dot{\hat{\mathbf{x}}}$ their derivatives. The pairs (A_i, C) are assumed to be observable. When the error dynamics $\dot{\hat{\mathbf{e}}} = \dot{\mathbf{x}} - \dot{\hat{\mathbf{x}}}$, where $\mathbf{e}$ is the estimation error, are asymptotically stable, an estimate of the real states is achieved. The stability conditions are given by Theorem 1. These stability conditions include a convergence rate $\alpha > 0$.

Theorem 1. *[30] The error dynamics $\dot{\hat{\mathbf{e}}}$ are asymptotically stable if there exists a common $P = P^T > 0$ such that,*

$$P(A_i - L_i C) + (P(A_i - L_i C))^T + 2\alpha P < 0, \qquad i = 1, \cdots, m \tag{4-20}$$

Remark. *With the change of variables $M_i = PL_i, \quad i = 1, \cdots, m$ Eq. (4-20) becomes Eq. (4-21)*

$$PA_i - M_i C + A_i^T P - C^T M_i^T + 2\alpha P < 0, \qquad i = 1, \cdots, m \tag{4-21}$$

The focus of this thesis lies on the performance of the observer, the control laws applied to this system can be found in [16].

4-3-3 Results

The Linear Matrix Inequality (LMI) problem in Theorem 1 was solved in Matlab using the function *feasp*. The resulting gain matrices are shown in Eq. (4-22).

$$L_1 = \begin{bmatrix} 63 \\ 3917.8 \\ 331.7 \end{bmatrix} \qquad L_2 = \begin{bmatrix} 45.6 \\ 2849.7 \\ 136.1 \end{bmatrix} \tag{4-22}$$

The system was run with an observer based feedback-linearisation control as shown in Beyhan et al. [16]. The results achieved are presented by the tracking and estimation performance in Figure 4-6 and the mass estimation in Figure 4-7.

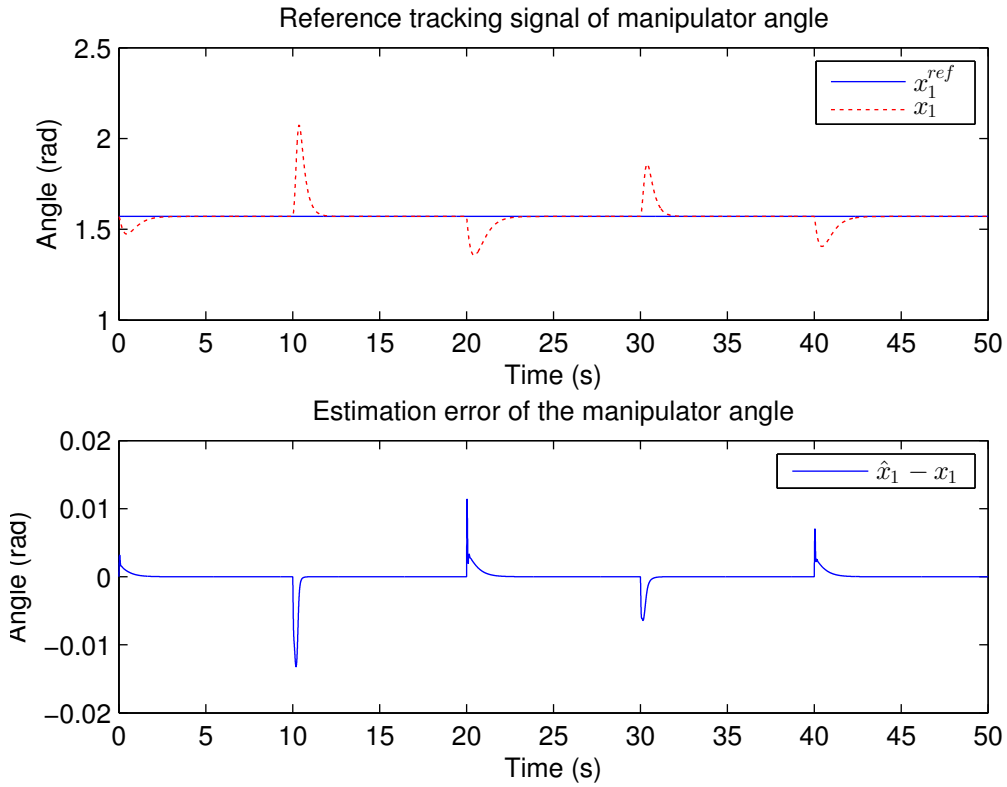

Figure 4-6: Tracking and estimation of manipulator angle

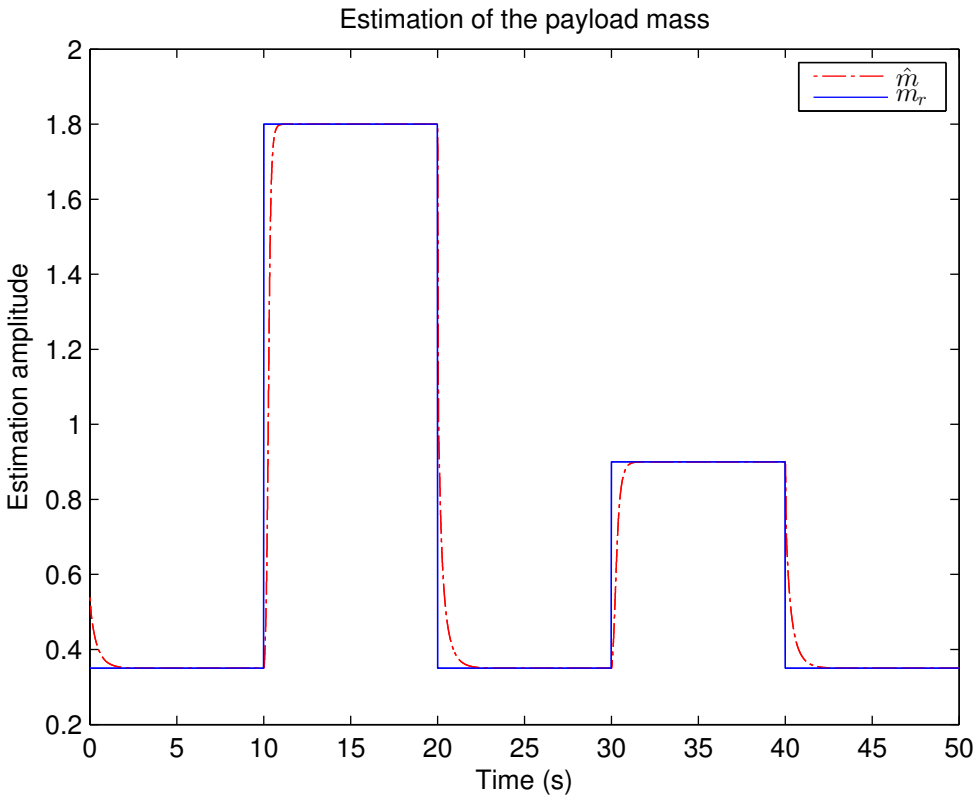

Figure 4-7: Estimation of payload mass

The results show that for a reference signal, which is a step towards $\frac{\pi}{2}$, on x_1, the arm holds steady and the estimation for the payload mass converges to the reference value shown by the blue line in Figure 4-7. This first result would offer a great opportunity for further development into Multi-Input Multi-Output (MIMO) systems and to apply to the framework of pHRI.

4-4 Example: Two-link manipulator

To develop the estimation performed by Beyhan et al. [16], the approach can be applied to the same two-link manipulator derived in Eq. (3-6). This representation can be rewritten into the general system in Eq. (4-8). As in the previously described example, the states of this system must be extended to include the payload mass for estimation. In Chapter 3 the chosen estimation included both mass estimates, and for this comparison the same approach will be used. Therefore, the state vector $\mathbf{x}$ must be extended for the two-link manipulator. The system as represented by Eq. (4-8) may be written out completely as shown in Eq. (4-23).

$$\begin{aligned} l_1^2\ddot{\phi}_1(m_1+m_2) - l_1 l_2 m_2(\dot{\phi}_2^2\sin(\phi_1-\phi_2) - \ddot{\phi}_2\cos(\phi_1-\phi_2)) &= \tau_1 \\ l_2^2 m_2\ddot{\phi}_2 + l_1 l_2 m_2\dot{\phi}_1^2\sin(\phi_1-\phi_2) + l_1 l_2 m_2\ddot{\phi}_1\cos(\phi_1-\phi_2) &= \tau_2 \end{aligned} \tag{4-23}$$

By choosing the extended state vector to be as defined in Eq. (4-24), the system can be rewritten into the general form in Eq. (4-8).

$$\mathbf{x} = \begin{bmatrix} \phi_1 \\ \phi_2 \\ \dot{\phi}_1 \\ \dot{\phi}_2 \\ m_2 \\ \frac{1}{m_1+m_2} \end{bmatrix} = \begin{bmatrix} x_1 \\ x_2 \\ x_3 \\ x_4 \\ x_5 \\ x_6 \end{bmatrix} \tag{4-24}$$

With these states, the two-link manipulator may be expressed in the form as shown in Eq. (4-25) where $u = [\tau_1, \tau_2]^T$, $\cos(x_1 - x_2) = c_{12}$ and $\sin(x_1 - x_2) = s_{12}$.

$$\begin{aligned} \dot{x}_3 &= \frac{-l_2\tau_1 x_6 - l_1\tau_2 x_6 c_{12} - l_1 l_2^2 x_4^2 x_5 x_6 s_{12} - l_1^2 l_2 x_3^2 x_5 x_6 s_{12} c_{12}}{l_1^2 l_2(x_5 x_6 c_{12}^2 - 1)} \\ \dot{x}_4 &= \frac{l_1\tau_2 + l_2\tau_1 x_5 x_6 c_{12} + l_1^2 l_2 x_3^2 x_5 s_{12} - l_1 l_2^2 x_4^2 x_5^2 x_6 s_{12} c_{12}}{l_1 l_2^2 x_5(x_5 x_6 c_{12}^2 - 1)} \end{aligned} \tag{4-25}$$

$$f(\mathbf{x}) = \begin{bmatrix} 0 & 0 & 1 & 0 & 0 & 0 \\ 0 & 0 & 0 & 1 & 0 & 0 \\ 0 & 0 & 0 & 0 & \frac{-l_1 l_2^2 x_4^2 x_6 s_{12}}{l_1^2 l_2(x_5 x_6 c_{12}^2 - 1)} & \frac{-l_1^2 l_2 x_3^2 x_5 s_{12} c_{12}}{l_1^2 l_2(x_5 x_6 c_{12}^2 - 1)} \\ 0 & 0 & 0 & 0 & \frac{l_1^2 l_2 x_3^2 s_{12}}{l_1 l_2^2 x_5(x_5 x_6 c_{12}^2 - 1)} & \frac{-l_1 l_2^2 x_4^2 x_5^2 s_{12} c_{12}}{l_1 l_2^2 x_5(x_5 x_6 c_{12}^2 - 1)} \\ 0 & 0 & 0 & 0 & 0 & 0 \\ 0 & 0 & 0 & 0 & 0 & 0 \end{bmatrix} \tag{4-26}$$

$$g(\mathbf{x}) = \begin{bmatrix} 0 & 0 \\ 0 & 0 \\ \frac{-l_2 x_6}{l_1^2 l_2 (x_5 x_6 c_{12}^2 - 1)} & \frac{-l_1 x_6 c_{12}}{l_1^2 l_2 (x_5 x_6 c_{12}^2 - 1)} \\ \frac{l_2 x_5 x_6 c_{12}}{l_1 l_2^2 x_5 (x_5 x_6 c_{12}^2 - 1)} & \frac{l_1}{l_1 l_2^2 x_5 (x_5 x_6 c_{12}^2 - 1)} \\ 0 & 0 \\ 0 & 0 \end{bmatrix} \tag{4-27}$$

It is assumed that for this two-link manipulator system only the angular positions (ϕ_1, ϕ_2) are measured, see Eq. (4-28).

$$\mathbf{y} = \begin{bmatrix} 1 & 0 & 0 & 0 & 0 & 0 \\ 0 & 1 & 0 & 0 & 0 & 0 \end{bmatrix} \mathbf{x} \tag{4-28}$$

This definition of the nonlinear matrix functions $f(\mathbf{x})$ and $g(\mathbf{x})$, allows the construction of the scheduling variables. Eq. (4-26) and Eq. (4-27) contain eight non-constant terms, each of which will be replaced by a scheduling variable. This means that a $\mathbf{z}$ vector may be defined as shown in Eq. (4-29)

$$\begin{aligned} \mathbf{z} &= [z_1, z_2, z_3, z_4, z_5, z_6, z_7, z_8]^T \\ z_1 &= \frac{-l_1 l_2^2 x_4^2 x_6 s_{12}}{l_1^2 l_2 (x_5 x_6 c_{12}^2 - 1)} \\ z_2 &= \frac{-l_1^2 l_2 x_3^2 x_5 s_{12} c_{12}}{l_1^2 l_2 (x_5 x_6 c_{12}^2 - 1)} \\ z_3 &= \frac{l_1^2 l_2 x_3^2 s_{12}}{l_1 l_2^2 x_5 (x_5 x_6 c_{12}^2 - 1)} \\ z_4 &= \frac{-l_1 l_2^2 x_4^2 x_5^2 s_{12} c_{12}}{l_1 l_2^2 x_5 (x_5 x_6 c_{12}^2 - 1)} \\ z_5 &= \frac{-l_2 x_6}{l_1^2 l_2 (x_5 x_6 c_{12}^2 - 1)} \\ z_6 &= \frac{-l_1 x_6 c_{12}}{l_1^2 l_2 (x_5 x_6 c_{12}^2 - 1)} \\ z_7 &= \frac{l_2 x_5 x_6 c_{12}}{l_1 l_2^2 x_5 (x_5 x_6 c_{12}^2 - 1)} \\ z_8 &= \frac{l_1}{l_1 l_2^2 x_5 (x_5 x_6 c_{12}^2 - 1)} \end{aligned} \tag{4-29}$$

A number of assumptions must be made regarding the maximum and minimum values of the states. For the two-link manipulator, the following maxima and minima will be used.

$$\begin{aligned} x_1 &\in \left[-\frac{\pi}{2}, \frac{\pi}{2}\right] \\ x_2 &\in \left[-\frac{\pi}{2}, \frac{\pi}{2}\right] \\ x_3 &\in [-2\pi, 2\pi] \\ x_4 &\in [-2\pi, 2\pi] \\ x_5 &\in [1, 5] \\ x_6 &\in \left[\frac{1}{2}, \frac{1}{10}\right] \end{aligned}$$

To find the maxima and minima of the scheduling variables, the z_j functions in Eq. (4-29) are analysed within the maxima and minima of the states. This results in the ranges for z_j shown in Eq. (4-30), assuming that $l_1 = 2$ and $l_2 = 3$.

$$\begin{aligned} z_1 &\in [-29.6088, 29.6088] \\ z_2 &\in [-241.7295, 241.7295] \\ z_3 &\in [-26.3189, 26.3189] \\ z_4 &\in [-241.7295, 241.7295] \\ z_5 &\in [0.025, 0.25] \\ z_6 &\in [-0.1667, 0.1667] \\ z_7 &\in [-0.1667, 0.1667] \\ z_8 &\in [-0.2222, -0.0222] \end{aligned} \tag{4-30}$$

The weighting functions of these scheduling variables may now be defined as shown in Table 4-1. The fuzzy models consist of the product of all each of the eight η_j functions. For each of the combinations a state space model can be constructed as demonstrated in Eq. (4-31) and Eq. (4-32).

$$\begin{aligned} w_1(\mathbf{z}) &= \eta_0^1 \eta_0^2 \eta_0^3 \eta_0^4 \eta_0^5 \eta_0^6 \eta_0^7 \eta_0^8 \\ \dot{\mathbf{x}} &= \begin{bmatrix} 0 & 0 & 1 & 0 & 0 & 0 \\ 0 & 0 & 0 & 1 & 0 & 0 \\ 0 & 0 & 0 & 0 & -29.6088 & -241.7295 \\ 0 & 0 & 0 & 0 & -26.31899 & -241.7295 \\ 0 & 0 & 0 & 0 & 0 & 0 \\ 0 & 0 & 0 & 0 & 0 & 0 \end{bmatrix} \mathbf{x} + \begin{bmatrix} 0 & 0 \\ 0 & 0 \\ 0.025 & -0.1667 \\ -0.1667 & -0.2222 \\ 0 & 0 \\ 0 & 0 \end{bmatrix} \mathbf{u} \end{aligned} \tag{4-31}$$

z_j	η_j^0	η_j^1
z_1	$\frac{29.6088-\frac{-l_1 l_2^2 x_4^2 x_6 s_{12}}{l_1^2 l_2 (x_5 x_6 c_{12}^2 - 1)}}{29.6088--29.6088}$	$1-\eta_1^0$
z_2	$\frac{241.7295-\frac{-l_1^2 l_2 x_3^2 x_5 s_{12} c_{12}}{l_1^2 l_2 (x_5 x_6 c_{12}^2 - 1)}}{241.7295--241.7295}$	$1-\eta_2^0$
z_3	$\frac{26.3189-\frac{l_1^2 l_2 x_3^2 s_{12}}{l_1 l_2^2 x_5 (x_5 x_6 c_{12}^2 - 1)}}{26.3189--26.3189}$	$1-\eta_3^0$
z_4	$\frac{241.7295-\frac{-l_1 l_2^2 x_4^2 x_5^2 s_{12} c_{12}}{l_1 l_2^2 x_5 (x_5 x_6 c_{12}^2 - 1)}}{241.7295--241.7295}$	$1-\eta_4^0$
z_5	$\frac{0.25-\frac{-l_2 x_6}{l_1^2 l_2 (x_5 x_6 c_{12}^2 - 1)}}{0.25-0.025}$	$1-\eta_5^0$
z_6	$\frac{0.1667-\frac{-l_1 x_6 c_{12}}{l_1^2 l_2 (x_5 x_6 c_{12}^2 - 1)}}{0.1667--0.1667}$	$1-\eta_6^0$
z_7	$\frac{0.1667-\frac{l_2 x_5 x_6 c_{12}}{l_1 l_2^2 x_5 (x_5 x_6 c_{12}^2 - 1)}}{0.1667--0.1667}$	$1-\eta_7^0$
z_8	$\frac{-0.0222-\frac{l_1}{l_1 l_2^2 x_5 (x_5 x_6 c_{12}^2 - 1)}}{-0.0222--0.2222}$	$1-\eta_8^0$

Table 4-1: Weighing functions

$$
\begin{aligned}
&w_1(\mathbf{z}) = \eta_1^1 \eta_0^2 \eta_0^3 \eta_0^4 \eta_0^5 \eta_0^6 \eta_0^7 \eta_0^8 \\
&\dot{\mathbf{x}} = \begin{bmatrix} 0 & 0 & 1 & 0 & 0 & 0 \\ 0 & 0 & 0 & 1 & 0 & 0 \\ 0 & 0 & 0 & 0 & 29.6088 & -241.7295 \\ 0 & 0 & 0 & 0 & -26.31899 & -241.7295 \\ 0 & 0 & 0 & 0 & 0 & 0 \\ 0 & 0 & 0 & 0 & 0 & 0 \end{bmatrix} \mathbf{x} + \begin{bmatrix} 0 & 0 \\ 0 & 0 \\ 0.025 & -0.1667 \\ -0.1667 & -0.2222 \\ 0 & 0 \\ 0 & 0 \end{bmatrix} \mathbf{u}
\end{aligned} \tag{4-32}
$$

There are in total 256 rules, and therefore 256 fuzzy models as those shown in Eq. (4-32). Now that the model has been explained, and since the outputs do not portray the entire state vector, the observability matrix for this system must be checked to find out whether an observer may allow the states to be estimated.

4-5 Observer Design: Estimated Scheduling Vector

For any functional observer, the combination of the A_i and C matrices must satisfy the observability criterion. The construction of an observer is highly dependent on whether the system matrices contain enough information about the system to infer the states from the outputs.

4-5-1 Observability

A Linear Time-Invariant (LTI) system may be said to be observable when the observability matrix ($\mathcal{O}_j$) is full row rank.

$$\mathcal{O}_j = \begin{bmatrix} C \\ CA_j \\ CA_j^2 \\ CA_j^3 \\ CA_j^4 \\ CA_j^5 \end{bmatrix}, \qquad j = 1, \cdots, r \tag{4-33}$$

The observability for all linear systems was found to be full row rank. This means that an observer can be developed to estimate the states.

4-5-2 Fuzzy Luenberger observer

The well known classical Luenberger observer [31] has been extended for fuzzy systems to become the fuzzy-Luenberger observer [28] [29]. This observer can be used when a fuzzy system uses a scheduling vector independent of the unmeasured states $\mathbf{z}$, and when it is dependent on the unmeasured states $\hat{\mathbf{z}}$. Due to the construction of the above described system, the observer for systems whose scheduling vector is dependent on unmeasured states must be used. An observer for this system is defined in Eq. (4-34).

$$\begin{aligned} \dot{\hat{\mathbf{x}}} &= \sum_{i=1}^{M} w_i(\hat{\mathbf{z}}_j) \left(A_i \hat{\mathbf{x}} + B_i \mathbf{u} + L_i(\mathbf{y} - \hat{\mathbf{y}}) \right) \\ \hat{\mathbf{y}} &= C\hat{\mathbf{x}} \end{aligned} \tag{4-34}$$

The error dynamics ($\mathbf{e} = \mathbf{x} - \mathbf{x}$) for such a system is defined by Eq. (4-35).

$$\dot{\mathbf{e}} = \sum_{i=1}^{m} w_i(\hat{\mathbf{z}}) \left(A_i - L_i C \right) \mathbf{e} + \sum_{i=1}^{m} (w_i(\mathbf{z}) - w_i(\hat{\mathbf{z}})) \left(A_i \mathbf{x} + B_i \mathbf{u} \right) \tag{4-35}$$

Due to the scheduling vector consisting of the estimated variables rather than system states, $\hat{\mathbf{z}}$ may be redefined for the example as shown in Eq. (4-36).

$$\hat{\mathbf{z}} = \begin{bmatrix} \hat{z}_1 \\ \hat{z}_2 \\ \hat{z}_3 \\ \hat{z}_4 \\ \hat{z}_5 \\ \hat{z}_6 \\ \hat{z}_7 \\ \hat{z}_8 \end{bmatrix} = \begin{bmatrix} \frac{-l_1 l_2^2 \hat{x}_4^2 \hat{x}_6 s_{12}}{l_1^2 l_2 (\hat{x}_5 \hat{x}_6 c_{12}^2 - 1)} \\ \frac{-l_1^2 l_2 \hat{x}_3^2 \hat{x}_5 s_{12} c_{12}}{l_1^2 l_2 (\hat{x}_5 \hat{x}_6 c_{12}^2 - 1)} \\ \frac{l_1^2 l_2 \hat{x}_3^2 s_{12}}{l_1 l_2^2 \hat{x}_5 (\hat{x}_5 \hat{x}_6 c_{12}^2 - 1)} \\ \frac{-l_1 l_2^2 \hat{x}_4^2 \hat{x}_5^2 s_{12} c_{12}}{l_1 l_2^2 \hat{x}_5 (\hat{x}_5 \hat{x}_6 c_{12}^2 - 1)} \\ \frac{-l_2 \hat{x}_6}{l_1^2 l_2 (\hat{x}_5 \hat{x}_6 c_{12}^2 - 1)} \\ \frac{-l_1 \hat{x}_6 c_{12}}{l_1^2 l_2 (\hat{x}_5 \hat{x}_6 c_{12}^2 - 1)} \\ \frac{l_2 \hat{x}_5 \hat{x}_6 c_{12}}{l_1 l_2^2 \hat{x}_5 (\hat{x}_5 \hat{x}_6 c_{12}^2 - 1)} \\ \frac{l_1}{l_1 l_2^2 \hat{x}_5 (\hat{x}_5 \hat{x}_6 c_{12}^2 - 1)} \end{bmatrix} \tag{4-36}$$

Bergsten [32] showed that for such a system, sufficient stability conditions are given by Theorem 2.

Theorem 2. *[32] Consider the error system in Eq. (4-35) and assume that*

$$\left\| \sum_{i=1}^{m} (w_i(\mathbf{z}) - w_i(\hat{\mathbf{z}}))\,(A_i\mathbf{x} + B_i\mathbf{u}) \right\| \leq \mu \left\| \mathbf{e} \right\| \tag{4-37}$$

where $\mu > 0$ is a known constant. Then, the error system is exponentially stable if there exists $P = P^T > 0$, $Q = Q^T > 0$ and $L_i, i = 1, 2, \cdots, m$ so that

$$\begin{aligned} P(A_i - L_iC) + (P(A_i - L_iC))^T &\leq -Q \\ \begin{bmatrix} Q - \mu^2 & P \\ P & I \end{bmatrix} &> 0 \end{aligned} \tag{4-38}$$

Remark. *With the change of variables $M_i = PL_i$, Eq. (4-38) becomes:*

$$PA_i - M_iC + A_i^T P - C^T M_i^T \leq -Q \tag{4-39}$$

which can be solved using the Yalmip toolbox for Matlab.

Remark. *As long as the membership functions are smooth and the variables are defined on a compact set, there exists a $\mu > 0$ so that Eq. (4-38) holds. The bounding constant μ in general can be found by solving the optimization problem [33].*

$$\mu = \max_{\mathbf{x},\mathbf{u},\hat{\mathbf{x}},\hat{\mathbf{z}}} = \left\| \frac{\partial (w_i(\mathbf{z}) - w_i(\hat{\mathbf{z}}))\,(A_i\mathbf{x} + B_i\mathbf{u})}{\partial \mathbf{e}} \right\|$$

4-5-3 Simulation results

Unfortunately, while the theory shows a feasible solution may exist for the error dynamics to be made exponentially stable, the Matlab toolbox is not able to find one. Regardless of the solver used to try to find a feasible solution, one cannot be found. To try another approach, the system can be simplified to include only the payload mass in the estimation procedure. The first mass in Eq. (4-23) is part of the robot arm, and can be assumed known. This would lower the number of scheduling parameters and states. Since the observer theory is still valid for such a system, only the sector nonlinearity approach needs to be recalculated.

4-6 Payload Mass Estimation

Starting again from Eq. (4-24) the state vector needs to be redefined to Eq. (4-40).

$$\mathbf{x} = \begin{bmatrix} \phi_1 \\ \phi_2 \\ \dot{\phi}_1 \\ \dot{\phi}_2 \\ m_2 \end{bmatrix} = \begin{bmatrix} x_1 \\ x_2 \\ x_3 \\ x_4 \\ x_5 \end{bmatrix} \tag{4-40}$$

With this state vector, the system may be described by Eq. (4-41) and Eq. (4-42).

$$\dot{x}_3 = \frac{x_5 c_{12} s_{12} l_1^2 l_2 x_3^2 + x_5 s_{12} l_1 l_2^2 x_4^2 - \tau_2 c_{12} l_1 + \tau_1 l_2}{l_1^2 l_2 (m_2 + x_5 - x_5 c_{12}^2)} \tag{4-41}$$

$$\dot{x}_4 = \frac{-s_{12} l_1^2 l_2 x_3^2 x_5^2 - m_2 s_{12} l_1^2 l_2 x_3^2 x_5 - c_{12} s_{12} l_1 l_2^2 x_4^2 x_5^2 + \tau_2 l_1 x_5 + m_2 \tau_2 l_1 - \tau_1 c_{12} l_2 x_5}{l_1 l_2^2 x_5 (m_2 + x_5 - x_5 c_{12}^2)} \tag{4-42}$$

The new equations result in the following general equations.

$$f(\mathbf{x}) = \begin{bmatrix} 0 & 0 & 1 & 0 & 0 \\ 0 & 0 & 0 & 1 & 0 \\ 0 & 0 & 0 & 0 & \frac{c_{12} s_{12} l_1^2 l_2 x_3^2 + s_{12} l_1 l_2^2 x_4^2}{l_1^2 l_2 (m_2 + x_5 - x_5 c_{12}^2)} \\ 0 & 0 & 0 & 0 & \frac{-s_{12} l_1^2 l_2 x_3^2 x_5 - m_2 s_{12} l_1^2 l_2 x_3^2 - c_{12} s_{12} l_1 l_2^2 x_4^2 x_5}{l_1 l_2^2 x_5 (m_2 + x_5 - x_5 c_{12}^2)} \\ 0 & 0 & 0 & 0 & 0 \end{bmatrix} \tag{4-43}$$

$$g(\mathbf{x}) = \begin{bmatrix} 0 & 0 \\ 0 & 0 \\ \frac{c_{12} l_1}{l_1^2 l_2 (m_2 + x_5 - x_5 c_{12}^2)} & \frac{l_2}{l_1^2 l_2 (m_2 + x_5 - x_5 c_{12}^2)} \\ \frac{c_{12} l_2 x_5}{l_1 l_2^2 x_5 (m_2 + x_5 - x_5 c_{12}^2)} & \frac{m_2 l_1 + l_1 x_5}{l_1 l_2^2 x_5 (m_2 + x_5 - x_5 c_{12}^2)} \\ 0 & 0 \end{bmatrix} \tag{4-44}$$

Therefore, the scheduling vector becomes Eq. (4-45).

$$\hat{\mathbf{z}} = \begin{bmatrix} \hat{z}_1 \\ \hat{z}_2 \\ \hat{z}_3 \\ \hat{z}_4 \\ \hat{z}_5 \\ \hat{z}_6 \end{bmatrix} = \begin{bmatrix} \frac{c_{12} s_{12} l_1^2 l_2 \hat{x}_3^2 + s_{12} l_1 l_2^2 \hat{x}_4^2}{l_1^2 l_2 (m_2 + \hat{x}_5 - \hat{x}_5 c_{12}^2)} \\ \frac{-s_{12} l_1^2 l_2 \hat{x}_3^2 \hat{x}_5 - m_2 s_{12} l_1^2 l_2 \hat{x}_3^2 - c_{12} s_{12} l_1 l_2^2 \hat{x}_4^2 \hat{x}_5}{l_1 l_2^2 \hat{x}_5 (m_2 + \hat{x}_5 - \hat{x}_5 c_{12}^2)} \\ \frac{c_{12} l_1}{l_1^2 l_2 (m_2 + \hat{x}_5 - \hat{x}_5 c_{12}^2)} \\ \frac{l_2}{l_1^2 l_2 (m_2 + \hat{x}_5 - \hat{x}_5 c_{12}^2)} \\ \frac{c_{12} l_2 \hat{x}_5}{l_1 l_2^2 \hat{x}_5 (m_2 + \hat{x}_5 - \hat{x}_5 c_{12}^2)} \\ \frac{m_2 l_1 + l_1 \hat{x}_5}{l_1 l_2^2 \hat{x}_5 (m_2 + \hat{x}_5 - \hat{x}_5 c_{12}^2)} \end{bmatrix} \tag{4-45}$$

The fuzzy system matrices may be defined using the scheduling variables as shown in Eq. (4-46)

$$A_i = \begin{bmatrix} 0 & 0 & 1 & 0 & 0 \\ 0 & 0 & 0 & 1 & 0 \\ 0 & 0 & 0 & 0 & z_1 \\ 0 & 0 & 0 & 0 & z_2 \\ 0 & 0 & 0 & 0 & 0 \end{bmatrix}, \qquad B_i = \begin{bmatrix} 0 & 0 \\ 0 & 0 \\ z_3 & z_4 \\ z_5 & z_6 \\ 0 & 0 \end{bmatrix}, \qquad C = \begin{bmatrix} 1 & 0 & 0 & 0 & 0 \\ 0 & 1 & 0 & 0 & 0 \end{bmatrix}, \tag{4-46}$$

With these system equations, the observability matrix is full row rank and therefore, the system is observable. Using the inequalities in Theorem 2, an optimal observer gain may be found. Unfortunately, the toolbox in YALMIP and the LMITool in Matlab do not manage to compute a feasible solution for this system either. While this does not mean that a solution does not exist, it does mean that it cannot be found using the Matlab toolboxes. The theory for this approach seems to be a great solution but as its not working for these conditions, alternatives must be analysed. One such alternative is a sliding mode observer.

4-7 Sliding Mode Observer

The sliding mode observer is a much studied observer form, but the method used in the fuzzy logic variation is based on the work of Tan and Edwards [34], Palm and Driankov [28], and Bergsten [32]. The fuzzy system may be extended to include unmatched uncertainties due to modelling/approximation errors using $D\zeta_1$ and $E\zeta_2$, giving the system shown in Eq. (4-47).

$$\begin{aligned}\dot{\mathbf{x}} &= \sum_{i=1}^{m} w_i(\mathbf{z}_j)\left(A_i\mathbf{x} + B_i\mathbf{u}\right) + D\zeta_1 \\ \mathbf{y} &= \sum_{i=1}^{m} w_i(\mathbf{z}_j)\left(C_i\mathbf{x}\right) + E\zeta_2\end{aligned} \tag{4-47}$$

The sliding mode system works for a transformed system with the properties in the following remark.

Remark. *There exists a linear change of coordinates $\theta = T\mathbf{x}$ such that,*

$$\bar{D} = TD = \begin{bmatrix} 0 \\ \bar{D}_2 \end{bmatrix} \qquad \textit{and} \qquad \bar{C} = CT^{-1} = \begin{bmatrix} 0 & I \end{bmatrix} \tag{4-48}$$

The new system matrices will become:

$$\bar{A}_i = TA_iT^{-1}, \qquad \bar{B}_i = TB_i, \qquad L_i = T^{-1}\bar{L}_i \tag{4-49}$$

An observer with this form is shown in Eq. (4-50).

$$\begin{aligned}\dot{\mathbf{x}} &= \sum_{i=1}^{m} w_i(\mathbf{z}_j)\left(A_i\mathbf{x} + B_i\mathbf{u} + L_i(\mathbf{y} - \hat{\mathbf{y}}) + L_iE\nu_2\right) + D\nu_1 \\ \mathbf{y} &= \sum_{i=1}^{m} w_i(\mathbf{z}_j)\left(C_i\mathbf{x}\right) + E\zeta_2\end{aligned} \tag{4-50}$$

Where ν_1 and ν_2 are the sliding mode conditions. The constraints concerning this sliding mode observer are shown in Theorem 3.

Theorem 3. *Let L_i and Ξ be structured as*

$$\bar{L}_i = \begin{bmatrix} \bar{L}_i^1 \\ \bar{L}_i^2 \end{bmatrix} \qquad \textit{and} \quad \Xi = \begin{bmatrix} \mathcal{N}_{\bar{D}_2}^T \\ 0 \end{bmatrix} \tag{4-51}$$

where $\mathcal{N}$ is a basis of the null space of $\bar{D}_2^T$ (if $\mathcal{N}_{\bar{D}_2} = \emptyset$ then $\Xi = 0$) and $P_1 = P_1^T$, $P_2 = P_2^T$, and $Q = Q^T > 0$ such that

$$\begin{aligned} \tilde{P}_1 + \tilde{P}_2 &> 0 \\ M_1^i E &= 0 \\ \bar{A}_i^T\tilde{P}_1 + \tilde{P}_1\bar{A}_i + \bar{A}_i^T\tilde{P}_2 + \tilde{P}_2\bar{A}_i - \bar{C}^T M_i^T - M_i\bar{C} &\leq -Q \\ \begin{bmatrix} Q - \mu^2 & \tilde{P}_1 + \tilde{P}_2 \\ \tilde{P}_1 + \tilde{P}_2 & I \end{bmatrix} &> 0 \end{aligned}$$

where,

$$\tilde{P}_1 = \begin{bmatrix} P_1 & 0 \\ 0 & P_2 \end{bmatrix} \tag{4-52}$$

and

$$\tilde{P}_2 = \begin{bmatrix} I & 0 \\ 0 & \Xi^T \end{bmatrix} \begin{bmatrix} 0 & P_3 \\ P_3^T & 0 \end{bmatrix} \begin{bmatrix} I & 0 \\ 0 & \Xi \end{bmatrix} \tag{4-53}$$

To solve this set of equations for the observer gain, the relationship in Eq. (4-54) must be solved.

$$M_i = P\bar{L}_i = \begin{bmatrix} P_1 & P_3\Xi \\ \Xi^T P_3^T & P_2 \end{bmatrix} \begin{bmatrix} \bar{L}_i^1 \\ \bar{L}_i^2 \end{bmatrix} = \begin{bmatrix} P_1\bar{L}_i^1 + P_3\Xi\bar{L}_i^2 \\ P_2\bar{L}_i^2 + \Xi^T P_3^T \bar{L}_i^1 \end{bmatrix} = \begin{bmatrix} M_i^1 \\ M_i^2 \end{bmatrix} \tag{4-54}$$

The observer gains may therefore be found using $\bar{L}_i = (\tilde{P}_1 + \tilde{P}_2)^{-1} M_i$. The observer stated in the original coordinates is found in Eq. (4-55) where $L_i = T^{-1}\bar{L}_i$.

$$\begin{aligned} \dot{\hat{\mathbf{x}}} &= \sum_{i=1}^{M} w_i(\hat{\mathbf{z}}_j) \left(A_i\hat{\mathbf{x}} + B_i\mathbf{u} + L_i(\mathbf{y} - \hat{\mathbf{y}}) + L_i E\nu_2 \right) + D\nu_1 \\ \hat{\mathbf{y}} &= C\hat{\mathbf{x}} \end{aligned} \tag{4-55}$$

For this system the matrices will be used for the estimation of the payload mass alone. The transformation matrix that satisfies the conditions specified in Eq. (4-48) is:

$$T = \begin{bmatrix} 0 & 0 & 0 & 0 & 1 \\ 1 & 0 & 0 & 0 & 0 \\ 0 & 1 & 0 & 0 & 0 \\ 0 & 0 & 1 & 0 & 0 \\ 0 & 0 & 0 & 1 & 0 \end{bmatrix}$$

For the conditions in Theorem 3 no feasible solution could be found. The infeasible solutions found for both observer options begs the question of observability. While the observability matrix may suggest the existence of a feasible observer for each local linear system, it does not confirm the observability of the entire nonlinear system. The reasons for not finding a feasible solution for the described system must be further analysed.

Chapter 5

Conclusion and recommendations

As no feasible solution can be found for the described systems, but the method has been proven to work, the observability of the fuzzy system must be scrutinized. While the pairs (A_i, C) for all the systems are observable for every linear model, this does not guarantee the observability of the nonlinear system. Often the observability of the local models is used to justify general observability. This assumption often works and results in feasible observer gains. One such an example is the paper by Beyhan et al. [16]. Each of the pairs (A_i, C) have been tested with the observability matrix and each one has full rank. Another example is in the paper by Palm and Driankov [28], and more recently Soulami et al. [35]. This lack of clarity of the definition of observability of Takagi-Sugeno (TS) fuzzy system, shows a necessity for a method to analyse this property. If the observability properties for TS fuzzy systems can be generalized, an approach can be constructed to find observer gains. One paper looking into the improved observability analysis of a TS fuzzy model is by Ho et al. [36]. They investigate a model with a slightly different system structure as shown in Eq. (5-1).

$$\begin{aligned} \dot{\mathbf{x}} &= (A_i + \Delta A_i)\mathbf{x} + (B_i + \Delta B_i)\mathbf{u} \\ \mathbf{y} &= (C_i + \Delta C_i)\mathbf{x} \end{aligned} \tag{5-1}$$

where,

- ΔA_i is the uncertainty matrix of the system matrix,
- ΔB_i is the uncertainty matrix of the input matrix,
- ΔC_i is the uncertainty matrix of the output matrix.

This approach presents the criterion for robust global observability. This may offer a step into analysing the overall observability conditions regarding fuzzy systems as they are presented in this thesis. The approach presented here may still offer a good alternative to the classical approach by Slotine and Li. The advantages it has with respect to avoiding the persistence of excitation conditions may prove to be very important for the success of physical Human-Robot

Interaction (pHRI). Finding a solution to this problem will be a big step towards the industrial implementation of human and robotic cooperation at Koninklijke Luchtvaart Maatschappij (KLM). There are many opportunities for modernisation and improvements, and the ability to palletize with the assistance of a robot is a unique and innovative concept. Before practical implementation of such a robot, a number of others areas must be investigated:

- Safety regarding the collaborative procedure,
- Collision avoidance schemes,
- Robot motion design,
  - Attached at the ceiling?
  - Attached to the floor?
  - On a beam?
  - On wheels?
- Gripper design for multiple payloads.

Each of these areas can be solved once the control framework is in place. While the conditions for observer design in this thesis have not proved to result in feasible observer gains, further research may find them and help with a big step towards estimating the payload properties for a design for KLM.

Bibliography

[1] M. Bronsing, "Klm cargo flow allocation optimization at schiphol," Master's thesis, TU Delft, December 2013.

[2] KLM Cargo SPL/A3, *Aircraft Handling Manual*, 6 ed., June 2013.

[3] KLM Cargo SPL/A3, *Aircraft Handling Manual 330-200*, 2 ed., March 2011.

[4] KLM Cargo SPL/A3, *Aircraft Handling Manual 330-300*, 1 ed., February 2012.

[5] KLM Cargo SPL/A3, *Aircraft Handling Manual 737-700*, 1 ed., December 2008.

[6] KLM Cargo SPL/A3, *Aircraft Handling Manual 737-800*, 1 ed., December 2008.

[7] KLM Cargo SPL/A3, *Aircraft Handling Manual 737-900*, 1 ed., December 2008.

[8] KLM Cargo SPL/A3, *Aircraft Handling Manual 747-400*, 1 ed., December 2008.

[9] KLM Cargo SPL/A3, *Aircraft Handling Manual 747-400 ERF*, 1 ed., December 2008.

[10] KLM Cargo SPL/A3, *Aircraft Handling Manual 777-200*, 1 ed., February 2014.

[11] KLM Cargo SPL/A3, *Aircraft Handling Manual 777-300*, 1 ed., February 2014.

[12] KLM Cargo SPL/A3, *Aircraft Handling Manual MD-11*, 1 ed., December 2008.

[13] P. Jonkers, "Basic tools uld opbouw," OTC KLM cargo Air France, 2011.

[14] "Robot-centered work cell." Robotics Bible, December 2011. http://www.roboticsbible.com/robot-centered-work-cell.html.

[15] D. van Dieten, "Fuzzy adaptive human-robot collaborative control with varying payloads," literature review, TU Delft, December 2014.

[16] S. Beyhan, Z. Lendek, F. E. Sarabi, and R. Babŭska, "Adaptive ts fuzzy payload estimation based control of siso nonlinear systems." In consideration, December 2014.

[17] "Amsterdam airport schiphol." Vanderlande. http://www.vanderlande.nl/nl/Bagageafhandeling/Referenties/Amsterdam-Airport-Schiphol.htm.

[18] A. Pil, "Schiphol innoveert zich naar 70 miljoen koffers per jaar." Mechatronica en Machinebouw, November 2011. http://www.robots.com/education/industrial-history.

[19] E. Ackerman, "Korean shipbuilder testing industrial exoskeletons for future cybernetic workforce." IEEE Spectrum, August 5. http://spectrum.ieee.org/automaton/robotics/industrial-robots/korean-shipbuilder-testing-industrial-exoskeletons-for-future-cybernetic-workforce.

[20] A. Mörtl, M. Lawitzky, A. Kucukyilmaz, M. Sezgin, C. Basdogan, and S. Hirche, "The role of roles: Physical cooperation between humans and robots," *The International Journal of Robotics Research*, 2012.

[21] M. Lawitzky, A. Mörtl, and S. Hirche, "Load sharing in human-robot cooperative manipulation," in *RO-MAN, 2010 IEEE*, pp. 185–191, IEEE, 2010.

[22] A. F. Salleh, R. Ikeura, S. Hayakawa, and H. Sawai, "Cooperative object transfer: Effect of observing different part of the object on the cooperative task smoothness," *Journal of Biomechanical Science and Engineering*, vol. 6, no. 4, pp. 343–360, 2011.

[23] F. Vijverstra, J. Kok, and I. Lammerts, "Direct, indirect and composite adaptive control of robot manipulators," masters thesis, Technische Universiteit Eindhoven, July 1992.

[24] J.-J. E. Slotine and W. Li, "Composite adaptive control of robot manipulators," *Automatica*, vol. 25, no. 4, pp. 509 – 519, 1989.

[25] Z. Lendek, T. M. Guerra, R. Babuŝka, and B. De Schutter, *Stability analysis and nonlinear observer design using Takagi-Sugeno fuzzy models*, vol. 262. Springer, 2010.

[26] T. Takagi and M. Sugeno, "Fuzzy identification of systems and its applications to modeling and control," *Systems, Man and Cybernetics, IEEE Transactions on*, vol. SMC-15, pp. 116–132, Jan 1985.

[27] H. Ohtake, K. Tanaka, and H. Wang, "Fuzzy modeling via sector nonlinearity concept," in *IFSA World Congress and 20th NAFIPS International Conference, 2001. Joint 9th*, vol. 1, pp. 127–132, July 2001.

[28] R. Palm and D. Driankov, "Towards a systematic analysis of fuzzy observers," in *Fuzzy Information Processing Society, 1999. NAFIPS. 18th International Conference of the North American*, pp. 179–183, Jul 1999.

[29] P. Bergsten and R. Palm, "Thau-luenberger observers for ts fuzzy systems," in *9th IEEE International Conference on Fuzzy Systems, FUZZ IEEE*, pp. 7–10, 2000.

[30] K. Tanaka and H. Wang, "Fuzzy regulators and fuzzy observers: a linear matrix inequality approach," in *Decision and Control, 1997., Proceedings of the 36th IEEE Conference on*, vol. 2, pp. 1315–1320 vol.2, Dec 1997.

[31] D. G. Luenberger, "Observers for multivariable systems," *Automatic Control, IEEE Transactions on*, vol. 11, no. 2, pp. 190–197, 1966.

[32] P. Bergsten, "Observers and controllers for takagi-sugeno fuzzy systems," 2001.

[33] H. K. Khalil, "Nonlinear systems, 3rd," *New Jewsey, Prentice Hall*, vol. 9, 2002.

[34] C. P. Tan and C. Edwards, "An lmi approach for designing sliding mode observers," *International Journal of Control*, vol. 74, no. 16, pp. 1559–1568, 2001.

[35] J. Soulami, A. El Assoudi, M. Essabre, M. Habibi, and E. El Yaagoubi, "Observer design for a class of nonlinear descriptor systems: A takagi-sugeno approach with unmeasurable premise variables," *Journal of Control Science and Engineering*, vol. 2015, 2015.

[36] W.-H. Ho, S.-H. Chen, J.-H. Chou, *et al.*, "Observability robustness of uncertain fuzzy-model-based control systems," *International Journal of Innovative Computing, Information and Control*, vol. 9, no. 2, pp. 805–819, 2013.

Glossary

List of Acronyms

AGV	Automatic Guided Vehicle
AHM	Aircraft Handling Manual
AMS	Amsterdam
DPPP	Distributors Package Packing Problem
EUR	Europe
ITR	Information-Oriented Control
KLM	Koninklijke Luchtvaart Maatschappij
LMI	Linear Matrix Inequality
LTI	Linear Time-Invariant
MIMO	Multi-Input Multi-Output
M-ULD	Mixed Unit Load Device
PCHS	Pallet/Container Handling System
pHRI	physical Human-Robot Interaction
RFID	Radio Frequency Identification
SISO	Single-Input Single-Output
SPL	Amsterdam Airport Schiphol
T-ULD	True Unit Load Device
TS	Takagi-Sugeno
TUM	Technische Universität München

TV	Transport Vehicle
ULD	Unit Load Device
VG1/FB1	Vrachtgebouw/Freightbuilding 1
VG2/FB2	Vrachtgebouw/Freightbuilding 2
VG3/FB3	Vrachtgebouw/Freightbuilding 3
WP1	Worldport 1
WP2	Worldport 2
WS	Work Station

List of Symbols

Greek Symbols

α	Convergence rate
$\ddot{\varphi}(t)$	The angular acceleration of the robot arm
ΔA_i	Uncertainty matrix in the system matrix
ΔB_i	Uncertainty matrix in the input matrix
ΔC_i	Uncertainty matrix in the output matrix
$\eta_0^j(\cdot)$	Minimum weighting function
$\eta_1^j(\cdot)$	Maximum weighting function
Λ	A constant positive definite matrix
$\lambda(t)$	Forgetting factor
λ_0	Maximum forgetting rate
μ	The bounding constant
$\mu_M(x)$	Membership value of value x in fuzzy set M
ν_1	Sliding mode condition
ν_2	Sliding mode condition
$\phi_1(t)$	Angle of first manipulator link
$\phi_2(t)$	Angle of second manipulator link
$\tau(t)$	Vector of torque inputs
$\varepsilon_t(t)$	Tracking error
$\varphi(t)$	The angle of the robot arm
$\varphi_i(\mathbf{z})$	The truth value based on premise variables

Letter Symbols

$\ddot{q}(t)$	Vector of generalized accelerations
$\ddot{q}_d(t)$	Desired trajectory of the generalized accelerations

$\ddot{q}_r(t)$	The reference acceleration
$\dot{\hat{\mathbf{x}}}$	The derivative of the estimated model states
$\dot{\mathbf{x}}$	The derivative of the state vector
$\dot{q}(t)$	Vector of generalized velocities
$\dot{q}_d(t)$	Desired trajectory of the generalized velocities
$\dot{q}_r(t)$	The reference velocity
$\hat{\mathbf{x}}$	The estimated model states
$\hat{\mathbf{y}}$	The estimated model output
$\hat{\mathbf{z}}$	The scheduling vector based on estimated states
$\hat{a}(t)$	The estimated payload and robot parameters
$\hat{C}(q(t), \dot{q}(t))$	Estimation of matrix of centripetal and coriolis torques
$\hat{G}(q(t))$	Estimation of vector with gravitational torques
$\hat{H}(q(t))$	Estimation of symmetric positive definite manipulator inertia matrix
$\mathbf{e}$	Estimation error
$\mathbf{f}_c$	The enviromental forces applied to the object
$\mathbf{M}_c$	The mass matrix of an object
$\mathbf{u}_c$	The external wrench on an object
$\mathbf{x}$	The state vector
$\mathbf{x}_c$	The configuration coordinates of the object
$\mathbf{y}$	Model output
$\mathbf{z}$	The vector of scheduling variables
$\mathcal{N}$	The basis of the null space
$\mathcal{O}_j$	The observability matrix
$\overline{nl}_j$	Maximum of z_j
$\underline{nl}_j$	Minimum of z_j
$a(t)$	Vector with payload and robot parameters
A_i	The i-th state matrix
$a_i(\mathbf{y})$	The affine terms
B_i	The i-th input matrix
$C(q(t), \dot{q}(t))$	Matrix of centripetal and coriolis torques
C_i	The i-th output matrix
d	Vertical project of the spring displacement
$D\zeta_1$	The matched uncertainty in the states
$e(t)$	Prediction error
$E\zeta_2$	The matched uncertainty in the outputs
$F(t)$	The driving force
$f_i(\mathbf{z})$	Consequent vector function
g	Acceleration due to gravity
$G(q(t))$	Vector with gravitational torques
$H(q(t))$	Symmetric positive definite manipulator inertia matrix

K	The spring constant
k_0	Upper bound of the gain matrix norm
k_1	Tuning parameter for adaptation speed
K_D	Constant positive definite matrix
L	The link length
l_1	Length of first manipulator link
l_2	Length of second manipulator link
L_i	The observer gains
m	The payload mass
m_1	Mass at the end of the first link
m_2	Mass at the end of the second link
m_e	Mass of the end-effector
$m_L(t)$	Payload mass
P	Positive definite matrix in Lyapunov function
$P(t)$	Time-varying positive definite gain matrix
$q(t)$	Vector of generalized coordinates
$q_d(t)$	Desired trajectory of the generalized coordinates
r	Length of the spring arm
$R(t)$	Uniformly positive definite weighting matrix
R^i	The i-th model rule
T	Transformation matrix
$w_i(\mathbf{z})$	The normalized membership function
$Y(q(t), \dot{q}(t), \ddot{q}(t))$	Nonlinear matrix function
Z_p^i	The antecedent fuzzy sets
z_p	A vector of antecedent variables